Coordination Chemistry Reviews
181 (1999) 61–120

COORDINATION
CHEMISTRY
REVIEWS

Layered double hydroxides (LDH) intercalated with metal coordination compounds and oxometalates

Vicente Rives [a,*], María Angeles Ulibarri [b]

[a] *Departamento de Química Inorgánica, Universidad de Salamanca, Salamanca, Spain*
[b] *Departamento de Química Inorgánica e Ingeniería Química, Facultad de Ciencias, Universidad de Córdoba, Córdoba, Spain*

Received 24 April 1998; received in revised form 11 September 1998

Contents

---

* Corresponding author. Tel.: +34-923-294400/1545; fax: +34-923-294574; e-mail: vrives@gugu.usal.es.

PII: S0010-8545(98)00216-1

Abstract

This paper reviews the synthesis, properties and applications of layered double hydroxides (LDHs), also known as anionic clays or hydrotalcite-like materials, containing intercalated anions constituted by metal complexes or oxometalates. After an introduction describing the main features of these compounds, emphasis is put on the synthesis methods, characterization and applications.

Keywords: Anionic clays; Hydrotalcite-like materials; Layered double hydroxides; LDH; Oxometalates; Anionic compounds of metal ions

---

1. Introduction

Layered double hydroxides (LDHs), also known as anionic clays, are a family of compounds which are deserving much attention in recent years ([1–3] and references therein). The structure of most of them corresponds to that of hydrotalcite, a natural magnesium–aluminum hydroxycarbonate, discovered in Sweden around 1842, which occurs in nature in foliated and contorned plates and/or fibrous masses. Its formula is $Mg_6Al_2(OH)_{16}CO_3 \cdot 4H_2O$, although due to the relationship between its structure and that of brucite, $Mg(OH)_2$, it is usually formulated as $[Mg_{0.75}Al_{0.25}(OH)_2](CO_3)_{0.125} \cdot 0.5H_2O$. Brucite shows the well-known CdI_2-type structure, i.e. an hexagonal close-packing of hydroxyl ions, with all octahedral sites every two interlayers occupied by Mg^{2+} ions. Partial Mg^{2+}/Al^{3+} substitution gives rise to positively charged layers, thus leading to location of anions in the unoccupied interlayers. In natural hydrotalcite these interlayer anions are carbonate, and water molecules also exist in the interlayer space. Stacking of the layers can be accomplished in two ways, leading to two polytypes with a rombohedral ($3R$ symmetry) or an hexagonal cell ($2H$ symmetry); hydrotalcite corresponds to symmetry $3R$, Fig. 1, while the $2H$ analogous is known as manasseite [2]. On the other hand, the electric charge of the layers and the interlayer ions is just the opposite of that found in silicate clays (cationic clays), and for all these reasons, these materials are usually known as layered double hydroxides (LDH), anionic clays or hydrotalcite-like materials.

As with cationic clays, the interlayer anions are easily exchanged, and carbonate has been exchanged for many different anions [4–9], including even hydroxyl groups (meixnerite). The nature of the layer cations can be also changed, and, although most of the studies reported in the literature refer to systems with M^{2+}/M^{3+} cations in the layers, other are known with M^{2+}/M^{4+} [10,11] or the rather well studied Li^{+}/Al^{3+} system [12]. The value of the M^{3+}/M^{2+} ratio is limited if pure materials are desired, and such a ratio, in addition to being important, also determines the concentration of interlayer anions.

Also as cationic clays, hydrotalcites can be pillared with polynuclear anions [1,13–17], although the thermal stability of anionic clays is markedly lower than that of cationic clays. Its thermal decomposition leads to mixed oxides.

An important feature of these hydrotalcites is that they can be obtained, in addition to direct synthesis from soluble salt precursors or by anionic exchange, by recovering of the layered structure, once a hydrotalcite has been calcined at moderate temperatures; this treatment leads to mostly amorphous materials, which, in contact with solutions containing anions, recover the layered structure, hosting the anions in the interlayer space.

Interest in hydrotalcites and derived materials arises from the widely use they can be given: catalysts or catalyst supports, processing of selective chemical nanoreactors, separation and membrane technology, filtration, scavenging and controlled release of anions, electroactive and photoactive materials, etc. [1].

Most of the applications correspond to the field of heterogeneous catalysis [3,18,19], where the choice of different metal cations (hydrotalcites have been also prepared containing two or more different M^{2+} or M^{3+} cations in the brucite-like layers) make these materials rather suitable for a fine modulation of chemical composition and hence catalytic properties. On the other hand, as the cations in hydrotalcites are well dispersed, heterogeneous catalysts obtained upon thermal decomposition usually show a high dispersion of the metal sites. The use of microporous and mesoporous molecular sieve materials in catalysis, including LDHs and pillared LDHs, has been recently reviewed [20].

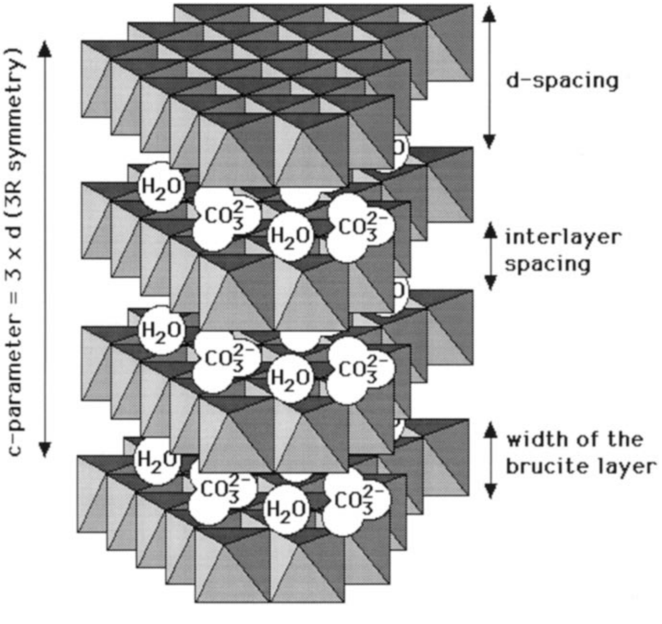

Fig. 1. Idealized structure of a layered double hydroxide, with interlayer carbonate anions. Several parameters are defined.

Intercalation of metal-containing anions in the interlayer space of hydrotalcites provides several advantages for an improved use: in the case of catalysts, it permits incorporation of, at least, a third metal component in the mixed oxide obtained upon thermal decomposition. In other materials, the interlayer space provides unique reaction conditions, thus permitting some reactions to take place under softer experimental conditions than in its absence.

In the present review we have collected the chemistry of hydrotalcite-like materials with metal-containing interlayer anions, well as halocomplexes, oxocomplexes, cyanocomplexes or oxometalates. In order to systematize the study, we have chosen a classification based on the nuclearity of the interlayer anion, rather than on the nature of the interlayer metal atom. Although we refer mostly on the preparation and characterization of these materials (and so experimental details are often given), changes induced in their properties (as compared with those displayed by the same anions in the bulk form), and their applications, are also considered. Literature until the end of 1997 has been reviewed.

2. Systems hosting single-metal anionic complexes

2.1. Layered double hydroxides intercalated with halocomplexes

LDHs intercalated with halo-complexes have been investigated as catalysts for chloride-exchange reactions, and also as modified electrodes. The reactivity of some halo-complexes in the interlayer space has been also investigated.

López-Salinas and Ono [21] have prepared Mg,Al–LDH with $[NiCl_4]^{2-}$ or $[CoCl_4]^{2-}$ in the interlayer by anion exchange (from a nitrate-containing precursor) in non-aqueous media. However, exchange is not complete (IR spectra of the LDH halo-complexes show a band at 1376 cm^{-1}, ascribed to mode ν_1 of NO_3^- anions), and the complexes partially decompose during the exchange process or the washing/drying steps. In addition, the IR spectra evidence the formation of a small amount of nickel nitrato-complexes, where the nitrato anions coordinate to nickel as bidentate ligands, as concluded from the positions of the ν_5 and ν_1 nitrate bands [22]. The nature of the non-aqueous solvent (ethanol or nitromethane) used during synthesis seems to play no major role on the nature of the interlayer species (for the Ni-compound), nor on the exchange degree (38% when synthesis was carried out in ethanol, and 26% in nitromethane).

The measured interlayer thickness of the LDH–MCl_4 (M = Ni, Co) compounds were almost coincident with that measured for the Mg,Al–NO_3 precursor, with the first (003) harmonic being recorded at 10.8 Å, corresponding to nitrate anions located in vertical position between the brucite-like layers [23]. Taking also into account that the interlayer width (3.3 Å) is smaller than the ionic diameter for $[NiCl_4]^{2-}$ in $[Me_4N]_2[NiCl_4]$, 4.6 Å [24], these findings throw some doubts about if the complex is located in the interlayer or simply adsorbed on the external surface. Outgassing of LDH–$CoCl_4$ at 200°C (a treatment that changed the color of the sample from green–blue to turquoise blue), and exposure to ammonia vapor, led to a change to a violet color, but the UV–vis bands expected for tetrahedral $[Co(NH_3)_4]^{2+}$ or octahedral $[Co(NH_3)_6]^{2+}$ species did not appear; instead, all the bands shifted to the high energy side of the spectrum. Gentle evacuation at room temperature (r.t.) restored the original spectrum, indicating that the interaction between ammonia and the Co(II) ions is rather weak. A similar experiment with pyridine (a stronger field ligand than ammonia in the spectrochemical series) gave rise to no color change, even after 1 week exposure at r.t. These results suggest pyridine does not reach the complex, which should be located in the interlayer space, and not simply adsorbed on the external surface of the particles.

UV–vis spectroscopy shows further evidence of reactivity in the interlayer space. In the solid state, the UV–vis/DR (Diffuse Reflectance) spectrum of the LDH–$[NiCl_4]$ compound prepared in ethanol shows, in addition to a doublet at 665 and 706 nm characteristic of $[NiEt_4]_2[NiCl_4]$ salt and of $[NiCl_4]^{2-}$ in solution, two bands at 550 and 750 nm that have been ascribed by these authors [21] to the presence of three-coordinated planar $[NiCl_3]^-$ species [25], while the presence of hexacoordinated Ni species, similar to those existing in $NiCl_2$ [26], can be concluded from the presence of a band at 450 nm.

In the interlayer space, chloride ligands in the coordination shell of Ni(II) ions can be reversibly exchanged by water molecules, as concluded from UV–vis/DR measurements. Outgassing the LDH–$[NiCl_4]$ compound under reduced pressure up to 150–250°C leads to development of bands characteristic of $[NiCl_4]^{2-}$ and $[NiCl_3]^-$, and the color of the sample changes from pale green to pale violet. These changes can be related to stripping of ligand molecules (residual water or solvent molecules) from hexacoordinated species $NiCl_4L_2$ ($L =$ ligand). Exposure of the outgassed solid to water vapor at r.t. results in a pale green solid, which spectrum shows a broad band at 700 nm and a weak band at 390 nm, which may be ascribed to $[Ni(H_2O)_6]^{2+}$ ions. Reevacuation at 200°C for 2 h results in a spectrum similar to that recorded before water adsorption, the pale-violet color being restored.

The green–blue colored Co-complex shows a somewhat different behavior. Its UV–vis/DR spectrum shows the characteristic split band at 610 and 658 nm, typical of tetrahedral Co(II) species, as in the precursor salt [27]; in addition, a broad feature at 500 nm suggests the presence of Co(II) species with a higher coordination number, probably $[Co(H_2O)_6]^{2+}$. Outgassing leads to a change in the color of the sample to turquoise blue, removal of the band at 500 nm, and shift of the split band to 570 and 608 nm, while a sharp band at 756 nm, with shoulders at 740 and 715 nm, develops. The anomalous position of the sharp band at 756 nm suggests, from comparison with the spectra of halo-cobalt(II) complexes (halide = Cl^-, Br^-, I^-) and other compounds, a decrease in the field strength around the Co(II) cation in evacuated LDH–$[CoCl_4]$. Exposure to water vapor removes the 756 nm band, suggesting formation of both tetrahedral and octahedral Co species, coordinated by chloride and aquo ligands, contrary to the results with the Ni analogous, where only octahedral species existed in the presence of water vapor.

Tetrachloronickelate(II) has been also introduced in the interlayer space of a Li,Al–LDH by anionic exchange from the nitrate form [28]. Again the interlayer space calculated (2.9 Å) from the spacing (7.7 Å) was too small for tetrahedral species. However, from EXAFS measurements, the first neighbor Ni–Cl distances were 2.10 Å, compatible with 4-fold coordination. In addition, no EPR signal was recorded for the LDH–[$NiCl_4$] compound, despite a strong signal was reported both for octahedral ($NiCl_2$) and tetrahedral ($[Et_4N]_2[NiCl_4]$ in nitromethane) species, thus suggesting that a change in the geometry has occurred in the LDH interlayer, forming square planar $[NiCl_4]^{2-}$ species which size, if the C_4 axis is perpendicular to the brucite-like layers, is compatible with the measured interlayer space.

The LDH–[$NiCl_4$] compound has been tested for chloride/bromide exchange in butyl bromide in toluene suspension [29]. The exchange rate has been found to be slightly lower than that for LDH in the chloride form. This rate sharply increases with the reaction temperature; thus, only 18% exchange was achieved at 50°C after 150 min, while at 100°C an exchange degree of 84% was reached; the reaction is inhibited in *n*-butanol and ethanol [30]. The exchanged bromide anion enters the coordination shell of interlayer Ni(II) ions, as concluded from UV–vis/DR results. This same compound, LDH[$NiCl_4$], also catalyzes the halide exchange reaction between benzyl chloride and butyl bromide [29,30], but only in DMF, and not in toluene.

Anion-exchanged hydrotalcite-like clay-modified electrodes containing $IrCl_6^{2-}$ in the interlayer have been reported by Itaya et al. [31]. These were prepared by anion exchange of the LDH in the chloride form (carbonate was not exchanged) by shaking the electrodes (films of LDH–Cl on SnO_2) with a 20 mM solution of the iridium complex for ca. 1 h, leading to a solid with a basal spacing of 10.8 Å, corresponding to an interlayer space of 6.03 Å. Steady voltammgrams recorded after an initial potential of 0 V (vs. SCE) for 10 s indicate that all $[IrCl_6]^{2-}$ ions incorporated into the film were reduced to $[IrCl_6]^{3-}$ at 0 V.

2.2. Layered double hydroxides intercalated with cyanocomplexes

Layered double hydroxides intercalated with cyano-complexes of iron, cobalt, molybdenum and some other metals have been synthesized and their properties for hydrocarbon adsorption and electrochemical behavior have been studied. In addition to X-ray diffraction, so useful to characterize these layered materials, IR and Mössbauer (in the case of iron and cobalt-containing cyanides) spectroscopies have been also widely used. The methods of synthesis used have been coprecipitation and anionic exchange in most of the cases, although reconstruction of the layered structure from a carbonate–LDH precursor calcined at 500°C has been also used [32].

Miyata and Hirose [33] reported the synthesis of a Mg,Al–$[Fe(CN)_6]^{4-}$ LDH by coprecipitation; its X-ray diffraction diagram is consistent with an hexagonal cell with $a = 3.06$ Å and $c = 33.62$ Å, i.e. the value for a is very close to that of the hydrotalcite with the same Mg/Al ratio, but the value for c has increased due to the larger ionic radii of hexacyanoferrate(II) with respect to that of carbonate. However, a small amount of carbonate also existed in the interlayer space, probably through adsorption from atmospheric carbon dioxide during preparation. Even so,

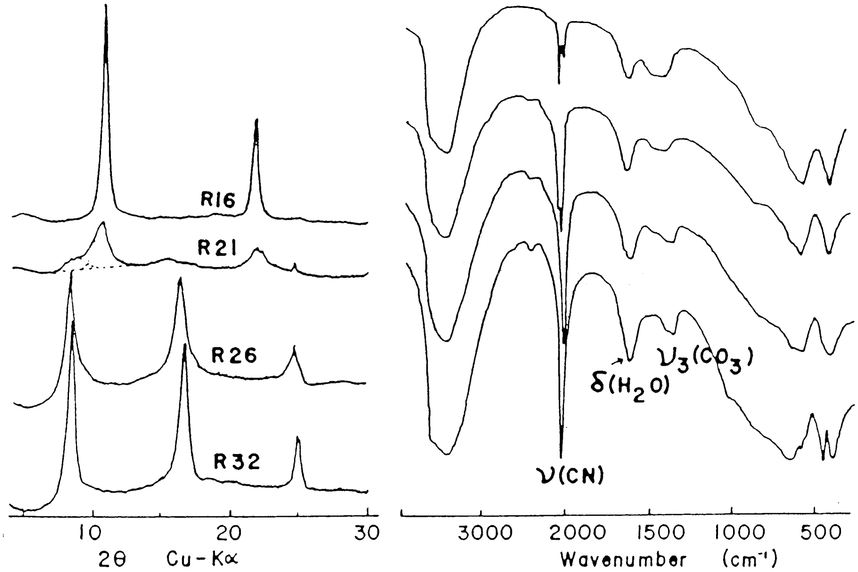

Fig. 2. X-ray powder diffractions and IR spectra of $[Fe(CN)_6]^{4-}$–LDH. R-values correspond to molar percentage of aluminum. Reprinted from S. Kikkawa, M. Koizumi, Ferrocyanide anion bearing Mg,Al hydroxide, Mater. Res. Bull. 17 (1982) 191–198, © 1982, with permission from Elsevier Science.

the amount of carbonate is markedly lower than that found as an impurity in hydrotalcites with monovalent anions, such as chloride or nitrate.

On heating, this material losses interlayer water continuously between 100 and 300°C, the thickness of the layer, *d*(003), decreasing from 11.18 to 8.04 Å at 250°C. At 300°C the material is almost amorphous, and at 400°C the layered structure collapses, with simultaneous removal of structural water (from condensation of layer hydroxyl groups) and decomposition of the interlayer anions. As observed with most of this sort of materials, nitrogen adsorption at -196°C for specific surface area assessment indicates its increase from 80 $m^2\ g^{-1}$ (original sample) to 348 $m^2\ g^{-1}$ for the sample calcined at 200°C, the maximum value (419 $m^2\ g^{-1}$) being measured for the sample calcined at 150°C. Once interlayer water molecules have been removed, interstitial sites in the interlayer are able to adsorb molecules such as O_2 or CO_2.

Similar compounds, but with varying Mg/Al ratios (between 2:1 and 5:1) have been prepared by Kikkawa and Koizumi [34], who have observed that intercalation of hexacyanoferrate(II) is favored as the Al content increases, especially for a Mg:Al ratio equal or lower than 3; for Mg:Al = 5:1 the major interlayer anion was carbonate and for intermediate values (Mg/Al = 4:1) both anions coexist, as concluded from the values for *d*(003) spacings, and also from the relative intensities of the IR bands recorded close to 2000 cm^{-1}, characteristic of ν(CN) in hexacyanoferrates [35] and the ν_3 band of carbonate close to 1350 cm^{-1}, Fig. 2.

One of the questions raised with these hexacyanoferrate-containing LDHs has been the orientation of the anion in the interlayer. In the case of carbonate it is widely accepted, from X-ray diffraction, ionic size and charge density, that its C_3 axis is perpendicular to the brucite-like layers, while in the case of nitrate it may be oriented with the C_3 axis parallel to the layers [23], due to the larger number of (monovalent) nitrate anions required to balance the positive charge of the layers, than of divalent carbonate anions; even for a Mg/Al ratio fairly low (i.e. with relatively high positive layers), a basal spacing of 8.8 Å (the same observed for a nitrate LDH) for a carbonate LDH, has been attributed to 'upright' oriented carbonate anions [36]. For hexacyanoferrate(II) LDHs, Kikkawa and Koizumi [34] suggest an orientation where the C_3 axis of the anion octahedron is perpendicular to the brucite-like layers, the face-to-face distance in the octahedron being 6.5 Å, thus leading to a total thickness of 11.3 Å (from the thickness of the brucite layer, 4.8 Å), a value fairly close to that determined by X-ray diffraction (ca. 11.2 Å), Fig. 3. This conclusion has been also reached by Braterman et al. [37] through a detailed study of the IR spectra of these compounds in the ν(CN) region using oriented and randomly oriented $[Mg_2Al(OH)_6]_4[Fe(CN)_6]$ (nominal composition) prepared by anionic exchange from a chloride-containing LDH. For a regular octahedron (O_h symmetry) with cyanide ligands in the corners, the C–N vibrational modes correspond to $A_{1g} + E_g + T_{1u}$. The first two modes are IR-forbidden, although they are recorded as very weak bands, and the band corresponding to mode T_{1u} splits into two bands, assigned to modes E_u and A_{2u}. These data support a decrease of symmetry from O_h to D_{3d}, with opposite triangular faces of the octahedron parallel to the brucite-like layers. In addition, the environment of the interlayer hexacyanoferrate anions is closer to that observed in aqueous solution than that observed in metallic salts, where the terminal nitrogen atom is bonded to a cation, so supporting a model where the anion becomes hydrogen-bonded to OH groups from the layers or from interlayer water molecules, but not directly bonded to Mg^{2+} or Al^{3+}. However, Wang et al. [38] attribute an interlayer spacing of 6.6 Å in an

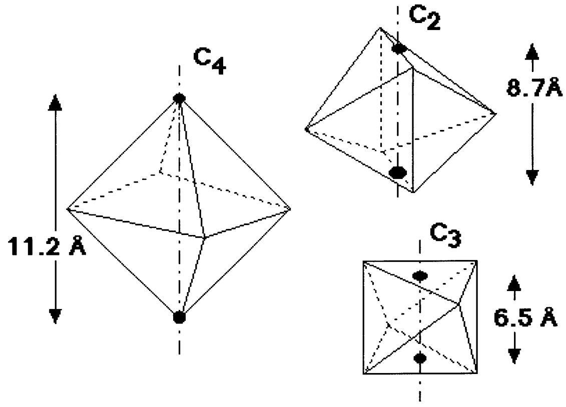

Fig. 3. Calculated end-to-end distances in a hexacyanoferrate ion octahedron. Adapted from Ref. [34].

hexacyanoferrate(III) Mg,Al–LDH prepared by direct synthesis to the octahedron oriented with its C_4 axis perpendicular to the brucite-like layers, although crystallographic data do not support his conclusion.

A decrease in the symmetry of the $[Fe(CN)_6]^{4-}$ octahedron in the interlayer space of $LiAl_2$–$[Fe(CN)_6]^{4-}$ (a material with a structure similar to that of hydrotalcite) prepared by ionic exchange of a chloride precursor, has been also concluded by Dutta and Puri [39] from its Raman and IR spectra, which shows five bands between 2094 and 2027 cm^{-1} (ν(CN) region) instead of the three bands at 2098 (Raman, A_{1g}), 2062 (Raman, E_g), and 2044 (IR, T_{1u}) cm^{-1} recorded in solution. As only four bands would be expected for a C_3 site symmetry, a lower symmetry or intermolecular coupling effects may be responsible for the spectrum observed.

The electronic state of iron in cyanoferrate-containing LDHs has been studied by IR and Mössbauer spectroscopies by Idemura et al. [40]. These authors have prepared different samples by anionic exchange of a nitrate–LDH (nominal Mg:Al ratio 3:1) with decarbonated water under nitrogen atmosphere with $K_3[Fe(CN)_6]$, $K_4[Fe(CN)_6]\cdot 3H_2O$, and $Na_2[Fe(CN)_5(NO)]\cdot 2H_2O$. Exchange with $[Fe(CN)_6]^{3-}$ reached only 84%, but its IR spectrum shows absorption bands at 2120 and 2040 cm^{-1}, due to ν(CN) of $[Fe(CN)_6]^{3-}$ and $[Fe(CN)_6]^{4-}$, respectively, suggesting a partial reduction from Fe(III) to Fe(II) during intercalation. When anionic exchange was carried out with $[Fe(CN)_6]^{4-}$, a single band was recorded at 2040 cm^{-1} if the sample had been dried under vacuum, but an additional band at 2120 cm^{-1} (characteristic of the hexacyanoferrate(III) complex) is recorded in addition when the sample was dried in air, i.e. partial Fe(II) → Fe(III) oxidation should take place. This behavior has been also observed in some other cases, although an unambiguous explanation is still lacking in the literature.

These redox processes have been also concluded from Mössbauer spectroscopy studies. Two different states for iron have been found in the $[Fe(CN)_6]^{3-}$ exchanged LDH: one corresponding to $[Fe(CN)_6]^{3-}$, although distorted along the C_3 axis, probably because of the stress from the host layers, and another corresponding to $[Fe(CN)_6]^{4-}$, formed upon reduction of hexacyanoferrate(III), although the mechanism for this reduction remains unclear. Correspondingly, the Mössbauer spectrum of the sample originally exchanged with $[Fe(CN)_6]^{4-}$ is identical to the second species above cited, confirming oxidation in this case.

The IR spectrum of the $[Fe(CN)s(NO)]^{2-}$ containing LDH shows an absorption at 1940 cm^{-1} (ν(NO) stretching) and four bands in the ν(CN) stretching region (2143–2040 cm^{-1}). From the relative intensities of the bands, if compared to those of the spectrum of the corresponding sodium salt, Idemura et al. conclude [40] that most of the NO ligands are removed along the exchange process. Detection of bands at 2040 and 2050 cm^{-1} (due to hexacyanoferrate(II)), together with the hexacyanoferrate(III) one at 2100 cm^{-1}, suggests a series of reactions in the layered host, as follows:

$$[Fe^{III}(CN)_5(NO)]^{2-} \rightarrow [Fe^{II}(CN)_5(NO)]^{3-} \rightarrow [Fe^{II}(CN)_5(NO)]^{3-} + NO \qquad (1)$$

$$[Fe^{II}(CN)_5]^{3-} + H_2O \rightarrow [Fe^{II}(CN)_5(H_2O)]^{3-} \rightarrow [Fe^{III}(CN)_5(H_2O)]^{2-} \qquad (2)$$

Carrado et al. [7] have found differences in the electronic properties of a Mg,Al–$[Fe(CN)_6]^{4-}$ LDH as synthetized (green crystals), or after being ground to a grey powder. In the former case, the Mössbauer spectrum shows isomer shifts of 1.8 and -0.14 mm s^{-1} (close to that of $K_3[Fe(CN)_6]$ at -0.124 mm s^{-1}), while the powder shows a single peak with an isomer shift of -0.13 mm s^{-1}, i.e. oxidation takes place already during synthesis, and is completed after grinding. These data have been confirmed by these same authors [7] by EPR, the spectra showing a signal near $g = 4.1$ due to Fe(III) in all cases. These results would suggest that the Fe(III)→Fe(II) reduction is achieved through pressure during grinding, and in fact, Larsen and Drickamer [41] have reported reduction of $K_3[Fe(CN)_6]$ under high pressure. On the other hand, in most cases reduction is concluded from IR spectra, where usually samples are prepared under high pressure as well in KBr pellets. However, IR spectra of Mg,Al–$[Fe(CN)_6]^{3-}$ LDHs recorded following the DRIFTS technique (where the samples are not submitted to high pressure) also show the presence of both oxidation states of iron [42].

Hansen and Koch [43] have synthetized a Mg,Al–$[Fe(CN)_6]^{4-}$ LDH from the carbonate form, via an intermediate nitrate form; carbonate is not completely expelled, and 30% of the layer positive charge is still balanced by interlayer carbonate. Partial oxidation (up to 20%) to $[Fe(CN)_6]^{3-}$ is also observed by these authors (as concluded from a IR spectroscopy study of the ν(CN) region and from Mössbauer spectroscopy studies) when the wet solid obtained during synthesis is dried in an oven at 70–100°C or is washed with oxygen-containing, non-aqueous solvents; however, if solvents without oxygen in their composition are used and the samples are dried at r.t., oxidation is prevented. These authors conclude that oxidation takes place not because of oxygen existing to the solvent molecule, but because of oxygen dissolved in ethanol or acetone, and when the solid is dried above r.t., the fast removal of water from the interlayer favors migration of oxygen to the interlayer space, where Fe(II) becomes oxidized. Miyata and Hirose [33] had previously reported that the interlayer space of a Mg,Al–$[Fe(CN)_6]^{4-}$ LDH is accesible to gases such as N_2 or O_2 after being dried at 100°C.

In any case, oxidation from Fe(II) to Fe(III) requires a change in the interlayer anions to keep balanced the positive charge of the brucite-like layers. These authors [43] also report that the IR band recorded at 2080 cm^{-1} is due to free cyanide ligands electrostatically held in the interlayer, and formed according to the reaction:

$$[Fe(CN)_6]^{4-} + H_2O \rightarrow [Fe(CN)_5(H_2O)]^{3-} + CN^- \qquad (3)$$

The IR band is not recorded in samples dried at 100°C, when water molecules are not available for such an exchange reaction, and the cyano–aquo complex is more prone to oxidation by dioxygen than the hexacyanoferrate(II) ion [44]. Attempts for a direct exchange to introduce cyanide anions in the interlayer, however, failed.

Hexacyanoferrate(II) and (III)-containing Mg,Al–LDHs have been also prepared by Holgado et al. [42] by ionic exchange of carbonate containing samples at pH 4.5 (with aqueous HCl), where intermediate exchange of chloride ions presumably takes place. The X-ray diffraction diagrams for these samples show two series of harmonics due to diffraction by (00l) planes, indicating the presence of mixed phases, with interlayer hexacyanoferrate and carbonate. Again, partial oxidation/reduction has been observed by these authors by IR spectroscopy, and their degree has been quantified from first derivative XANES spectra, concluding that 30% of Fe(II) becomes oxidized, while 20% of Fe(III) is reduced. When the samples are calcined in air at 600°C, X-ray diffraction and temperature-programmed reduction results suggest formation of MgO and $MgFe_2O_4$, whichever the starting hexacyanoferrate ((II) or (III))-containing LDH.

Crespo et al. [45] have reported a careful study of different methods (including direct synthesis, reconstruction from a calcined precursor, anionic exchange of a nitrate LDH, and via intermediate terephthalate) to prepare Zn,Al–LDH with hexacyanoferrate(II) and hexacyanoferrate (III). Although in all methods used, the redox process above observed also develops, these authors report that to obtain carbonate-free phases the best method was direct synthesis for hexacyanoferrate(II), while anionic exchange of a nitrate precursor for hexacyanoferrate(III).

Hexacyanocobaltate(III) anions have been introduced in the interlayer space of LDHs with different layer cations (Mg, Zn, Al, Cr) by anionic exchange of precursors with different anions (nitrate, sulphate, chloride, chromate) [46]. Exchange levels of 79–90% were reached in all cases, except for Zn,Cr–NO_3, where it was only 21%. The expansion of the interlayer space from 3.0–4.0 Å (depending on the precursor anion) to 6.0–6.5 Å suggests the $[Co(CN)_6]^{3-}$ anions are oriented with their C_3 axis perpendicular to the brucite-like layers, as previously reported for hexacyanoferrate complexes. Expansion of the interlayer space allows also access of nitrogen molecules during specific surface area measurements, which shows a value of 13 $m^2\ g^{-1}$ for the Mg,Al–NO_3 precursor, but 330 $m^2\ g^{-1}$ for the exchanged LDH. A similar increase in the specific surface area had been also reported by Cavalcanti et al. [47] for a $[Fe(CN)_6]^{3-}$ containing LDH. In addition, the shape of the isotherm changes from type II in the IUPAC classification [48], due to adsorption on non-porous solids, to a Langmuir type isotherm [47,49], due to adsorption on microporous solids. Expansion makes also the interlayer space accessible to linear hydrocarbons and, in a lesser extent, to branched hydrocarbons.

The accessibility of the interlayer space of hexacyanoferrate (both Fe(II) and Fe(III))-intercalated LDHs has been studied by Cavalcanti et al. [47]. For a given Mg/Al ratio (3.0), the population of $[Fe(CN)_6]^{4-}$ should be lower than that of $[Fe(CN)_6]^{3-}$ (because of the larger formal negative charge in the former), and thus, taking into account the close size of both anions, the void interlayer space accesible for adsorption would be larger. However, the measured specific surface areas were 246 $m^2\ g^{-1}$ for the $[Fe(CN)_6]^{4-}$–LDH, and 355 $m^2\ g^{-1}$ for the $[Fe(CN)_6]^{3-}$–LDH. This unexpected result is explained on the basis of the redox process occurring in these materials, as concluded from IR spectroscopy studies, and widely discussed above, as well as by incorporation of carbonate anions from the atmosphere to the interlayer space, for charge balance after such redox process. Results on adsorption of hydrocarbons (C_5–C_7) is consistent with the specific surface area values measured, and changes in the Mg/Al ratio are also consistent with a decrease in void interlayer space as the Al content is decreased. A variation in the charge density of the layers in Mg,Al–$[Fe(CN)_6]$ LDHs via the M^{2+}/M^{3+} ratio optimizes the porosity properties [50], with a value of 499 $m^2\ g^{-1}$ for a M^{2+}/M^{3+} ratio of 3.33.

The change in the capacity for carbon dioxide adsorption on a Mg,Al-$[Fe(CN)_6]^{4-}$ LDH with the Mg/Al ratio (between 1 and 7) has been studied by Mao et al. [51]. Maximum adsorption was observed for Mg:Al = 1.7, i.e. it depends not only on the width of the interlayer space (ranging, although not steadily, from 10.64 to 10.96 Å), but also on the layer charge. The isosteric heat of adsorption was calculated to be 43.3 kJ mol^{-1}, a value similar to that reported by Miyata and Hirose [33], who found the adsorption capacity for CO_2 of a Mg,Al–$[Fe(CN)_6]^{4-}$ LDH to be 60% of that of zeolite 5A [52].

The interlayer space of LDHs provides a reaction medium for chemical reactions. However, its utility is limited because of the interlayer space and the size of the reagents. So, reactions have been studied on LDHs previously expanded with large anions, such as hexacyanoferrates or terephthalate. Challier and Slade [53] have reported the oxidative (due to Cu^{2+}) polymerization of aniline between the layers of a Cu,Al–$[Fe(CN)_6]^{4-}$ LDH.

Metalocyano-containing LDHs have been also used to prepare modified electrodes, as the redox behavior of the interlayer anions makes them electrochemically active. Itaya et al. [31] have reported on LDHs containing $[Mo(CN)_8]^{4-}$ or $[Fe(CN)_6]^{3-}$ prepared by anionic exchange of a commercial Mg,Al–Cl precursor. A film (thickness ca. 100 nm) of the chloride hydrotalcite was prepared on SnO_2, and exchange was achieved by shaking the electrodes in dilute (20 mM) solutions of the metalocyano complexes. Interlayer spacings of 11.2 Å were measured, in agreement with previous results described above. The peak currents for the $[Mo(CN)_8]^{4-/3-}$ couple incorporated in the interlayer are clearly observed at ca. 0.5 V (vs. SCE), which is almost in complete agreement with the half-wave potential of this couple in the same solution. In addition, a steady voltammogram was obtained after 10–20 cycles, without further decrease after 60 min cycling, indicating the anion is strongly held in the interlayer space of the LDH. Similar results were obtained for $[Fe(CN)_6]^{3-}$.

Hexacyanoferrate(III) was used by Shaw et al. [54] as an electroactive probe to determine the availability of Zn^{2+} and Al^{3+} at the surface of a Zn,Al–Cl LDH applied at the surface of a glassy carbon electrode. When $[Fe(CN)_6]^{3-}$ is reduced at the electrode surface to $[Fe(CN)_6]^{4-}$, this becomes anchored forming a multilayered Prussian blue-like film, the nitrogen atom binding to Zn^{2+} and Al^{3+} ions from the layers (as concluded from XPS measurements for the N(1s) energy level), so demonstrating such an availability. Phenol was not electro-oxidized on this electrode, while such an oxidation was observed on the Mg,Al analogue, where the Prussian blue-like layer was not formed. From these results, and taking into account that oxidation of phenol is pH-dependent, these authors were able to assign effective pH values of >11.2 and 8.3, respectively, for the surfaces of Mg,Al–Cl and Zn,Al–Cl.

Hexacyanoferrate(II) modified carbon paste electrodes have been also studied by Labuda and Hudáková [55], who observe oxidation of ascorbic acid at a potential 0.4 V less positive than the oxidation potential at a bare carbon paste electrode, at

$pH > 4$. According to these authors, this electrode is more sensitive and more selective than carbon paste electrodes modified with organic salts and that hexacyanoferrate(II) bound to poly(4-vinylpyridine), and permits good storage and operational stability.

Qiu and Villemure [56] have found an enhanced reduction current when $[Fe(CN)_6]^{4-}$ or $[Mo(CN)_8]^{4-}$ are exchanged in Ni,Al or Ni,Fe–LDH-modified electrodes. These authors found that Ni^{2+} in these LDHs can be oxidized up to 4+ if sufficiently positive potentials are used, but they can be reduced only to 2.7+; reversible reduction to 2+ is attained only up to a maximum oxidation value of 3.6+, the layered structure being stable, at least, as far as X-ray diffraction diagram concerns. The enhancement in the cathodic current has been attributed to electron transfer between the intercalated anions and the oxidized Ni sites in the brucite-like layer, as no enhancement was observed when the oxidized forms of the cyanocomplexes were intercalated. Similar results were obtained in systems containing Mn or Co in the brucite-like layers, the voltammetric waves being smaller, however, if the interlayer anions were carbonate or chloride, instead of $[Fe(CN)_6]^{4-}$, $[Mo(CN)_8]^{4-}$ or $[Ru(CN)_6]^{4-}$. When the potentials of Ni, Co or Mn LDH modified electrodes were scanned in mixtures of the iron and ruthenium or molybdenum cyanocomplexes, electron transfer from $[Fe(CN)_6]^{4-}$ to electrochemically oxidized $[Ru(CN)_6]^{3-}$ or $[Mo(CN)_8]^{3-}$, mediated by the LDH electroactive metal centres, was observed, but such a transfer was not observed for the redox inactive Zn,Al–Cl LDH.

2.3. Layered double hydroxides intercalated with oxocomplexes

Corma et al. have reported the preparation of Zn,Al–LDHs containing Mo oxo-complexes in the interlayer, and their role as heterogeneous catalysts for the oxidation of thiols [57–60]. $[Mo^{VI}O_2(O_2CC(S)Ph_2)_2]^{2-}$ ($[O_2CC(S)Ph_2]^{2-}$ being the sterically hindered 2,2-diphenyl-2-mercaptoethanoate ligand) is able to oxidize aliphatic thiols under homogeneous conditions [61,62], it being reduced to a monomeric complex $[Mo^{V}O(O_2CC(S)Ph_2)_2]^{-}$. However, this is clearly a disadvantage, as this second complex does not undergo oxidation with Me_2SO, so cancelling the possibility to design catalytic cycles.

Reduction of the $Mo^{VI}O_2$ complex takes place [63] through Reactions (4), reduction by the thiol substrate, and (5), comproportionation of the $Mo^{VI}O_2$ species and its $Mo^{IV}O$ reduced form, to yield a $Mo^{V}O$ species:

$$[Mo^{VI}O_2\{O_2CC(S)Ph_2\}_2]^{2-} + 2R\text{–}SH \rightarrow [Mo^{IV}O\{O_2CC(S)Ph_2\}_2]^{2-} + RS\text{–}Sr + H_2O \quad (4)$$

$$[Mo^{VI}O_2\{O_2CC(S)Ph_2\}_2]^{2-} + [Mo^{IV}O\{O_2CC(S)Ph_2\}_2]^{2-} + 2H^+ \rightarrow 2[Mo^{V}O\{O_2CC(S)Ph_2\}_2]^{-} + H_2O \quad (5)$$

So, immobilization of the Mo complex in the interlayer space of an LDH prevents from Reaction (5) to take place, due to steric hinderance, and thus

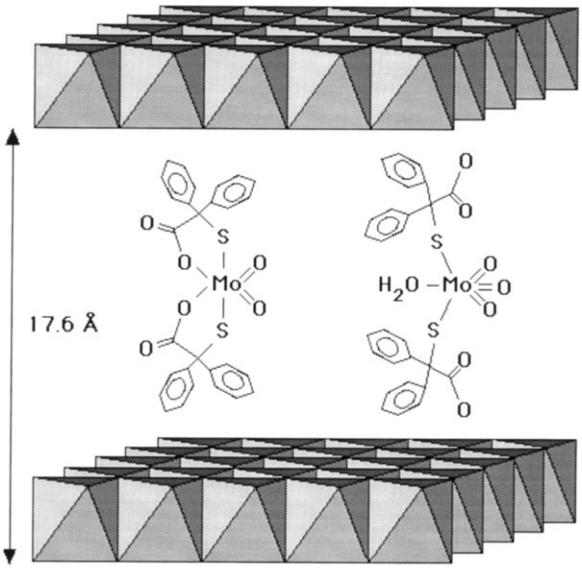

Fig. 4. Structure of intercalated $[MoO_2\{O_2CC(S)Ph_2\}_2]^{2-}$ based on basal spacing measurements (left), and from EXAFS results (right). Adapted from Ref. [60].

permiting species $[Mo^{IV}O\{O_2CC(S)Ph_2\}_2]^{2-}$ to be oxidized to close a catalytic cycle [59].

The LDH–Mo^{VI} intercalation compound was prepared by anionic exchange of the LDH in its nitrate form. The measured spacing for the (00l) reflection was 17.6 Å, corresponding to an interlayer space close to 13 Å, consistent with the anionic complex oriented with its C_2 axis parallel to the brucite-like layers; actually, the size of the anion in the direction perpendicular to such a C_2 axis was calculated to be 12.6 Å from X-ray crystallography [61]. Exchange, however, is not complete, as concluded from a FT-IR band at 1367 cm^{-1}, due to nitrate species (mode ν_3). The LDH–Mo^{VI} complex could not be obtained through the so-called reconstruction method. It is worthwhile to be mentioned that the intercalation compound is indefinitely stable in air.

The complex was active for thiophenol oxidation to disulphide by dioxygen, and the conversion was much lower when using air as the oxidizing agent. According to these authors [58], a catalytic cycle can be proposed, where the coupling of electron and proton transfer allows a direct formation of products without the formation of less stable intermediates, which would then have to be protonated by hydrolysis. Moreover, another advantage is the use of water as solvent.

Although X-ray diffraction and IR and UV–vis/DR spectroscopies data are consistent with the structure shown in Fig. 4(left), recent results [60] obtained by XAS indicate a change in the local coordination around the Mo^{VI} ions, as shown in Fig. 4(right) (both situations would lead, however, to similar values for the height of the interlayer space), from the isolated compound, to the situation when intercalated in the Zn,Al–LDH. The increase in the number of terminal oxygen atoms bonded to the Mo^{VI} ion, as concluded from XANES studies [60], follows decoordination of the carboxylate ligands, this being the first step which induces sufficient positive charge on the Mo^{VI} site to allow an oxygen atom transfer from a contiguous water molecule without any change in the oxidation state of Mo.

Mg,Al–LDH has been also intercalated with peroxomolybdate(VI) anions containing tartrate as ligand [64], $[Mo_2O_2(O_2)_4(C_4H_2O_6)]^{4-}$. Intercalation was achieved after swelling the LDH with terephthalate, a method widely used to intercalate large anions [65], leading to samples with spacings of 12.4 and 14.3 Å, respectively, for the terephthalate and peroxomolybdate-containing compounds. When suspended in water, this compound releases the peroxo group at 80°C to yield oxomolybdate, the process being reversible by addition of hydrogen peroxide; oxygen is released when heated in the solid state at ca. 120°C.

Pinnavaia et al. [66] have studied the effect of intercalation in different hosts on the properties of the excited-state of dioxorhenium(V) ions. From previous studies with polypyridyl complexes, it was concluded that the excited-state properties are preserved upon intercalation [67–70]. However, in the case of metal–oxo compounds and, particularly, d^2 *trans*-dioxo species [71], it was expected that its location in the interlayer space of LDHs and layered silicate clays would probably modify the orientation of the *trans*-ReO_2^+ core, thus affecting luminiscence properties. A Mg,Al–$ReO_2(CN)_4$ LDH was prepared by coprecipitation of the hydrotalcite in the presence of the complex anion, while intercalates in layered silicate clays were prepared with $[ReO_2py_4]^+$ and $[ReO_2en_2]^+$ (py = pyridine; en = ethylendiamine) in hectorite and fluorhectorite. In all three cases, exchange corresponded to ca. 15% of the exchange capacity of the clay.

Location of these complexes in the interlayer space of the clays gives rise only to minor structural distortions, as revealed by IR and Raman (in the resonance Raman effect mode) spectroscopies. Basal spacings (from XRD studies) are enlarged, consistenly with incorporation of the complexes. The luminescent hectorite intercalate is largely unperturbed, emission from the fluorhectorite intercalate is significantly attenuated, and no luminiscence was observed from the ReO_2–LDH intercalate. From basal spacing measurements and calculations of charge density of the layers, these differences have been related by these authors [66] to the different possibilities of orientation of the ReO_2 complexes in the interlayer space, Fig. 5. So, in the case of the hectorite intercalate, the complex should be located with its O–Re–O axis perpendicular to the layers, and the oxygen atoms can then be 'keyed' in the hexagonal cavities of the layered silicate clay; for the fluorhectorite intercalate, the higher charge density (27 vs. 80 Å^2 per charge unit for hectorite) precludes such an orientation, but data are consistent with the complex oriented with its C_4 axis parallel to the layers. Finally, for the LDH intercalate, the d-spacing is consistent with the effective C_3 axis of the pesudooctahedral $ReO_2(CN)_4^{3-}$ complex perpendicular to the layers, in agreement with previous studies which have demonstrated that the preferred orientation of intercalated anions in LDHs either maximizes the hydrogen bonding interactions of the protons of the brucite-like layers with the guest species, and/or minimizes the charge separation distance between the positive layers and the gallery anions [33,72,73]. Contrary to the structure of hectorite, in LDHs there are no cavities in which the ReO_2^+ core can key, and oxygen atoms of this core are probably hydrogen-bonded directly to the hydroxide layer. Because proton-donating solvent effects efficiently quench ReO_2^+ excited states by hydrogen bonding interactions [74], the non-radiactive decay rates of electronically-excited $ReO_2(CN)_4^{3-}$ ions in LDH are expected to be exceedingly fast.

2.4. Layered double hydroxides intercalated with macrocyclic ligand-containing complexes

One of systems most widely studied in recent years concerning LDHs, corresponds to those where the interlayer anion is a coordination compound with macrocyclic ligands; also, where the interlayer anion is the anionic ligand itself. These nanocomposite materials prepared with intercalated metalloporphyrines and

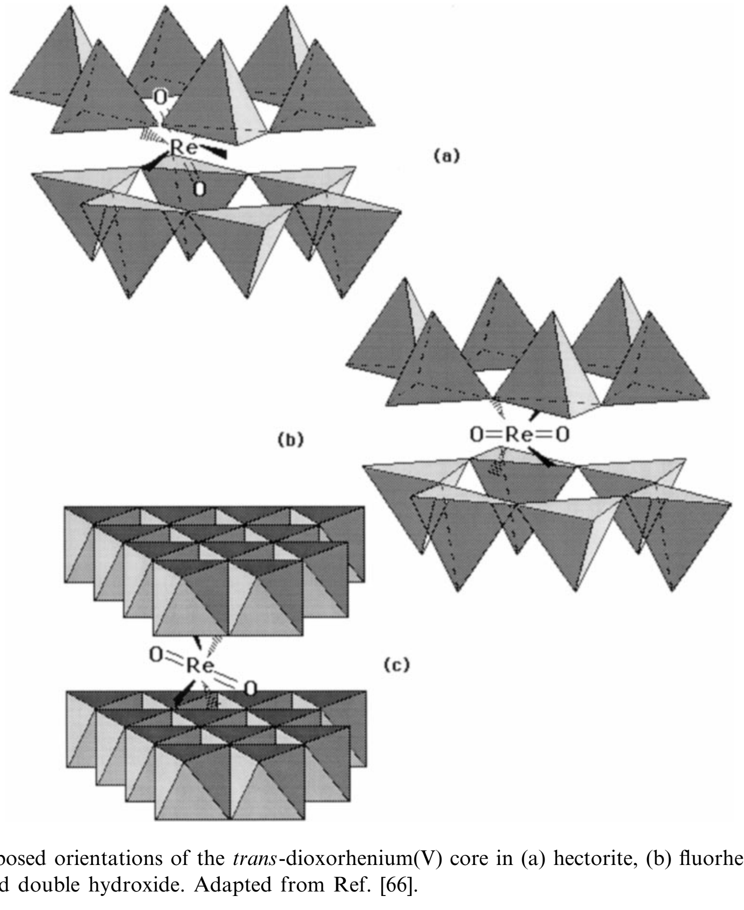

Fig. 5. Proposed orientations of the *trans*-dioxorhenium(V) core in (a) hectorite, (b) fluorhectorite, and (c) a layered double hydroxide. Adapted from Ref. [66].

metallophtalocyanines have shown interesting properties as heterogeneous catalysts for alkane hydroxylation, alkane epoxidation, alcohol and hydrocarbon oxidation [75–80]. They find also applications as electrochemical microsensors in the form of clay modified electrodes or as gas or optical sensors [81,82]. On the other hand, stacked metal-over-metal structures of phtalocyanines are being also studied as conducting materials [83], and the interlayer space of the LDHs provides a unique location for such a stacking arrangement. A review has been recently published on these [84] and related systems with other layered hosts [85], and their role as biomimetic catalysts.

One of the first papers [86] corresponds to the intercalation of 5,10,15,20-tetra(4-sulfonatephenyl)porphyrin (TSPP) in a Mg,Al–LDH. The interest of this anion arises from the high temperature photochemical hole burning (PHB) of its sodium salt above liquid nitrogen in a polyvinyl alcohol matrix [87], thus leading to investigations about the interaction of the anion with different host substances from the point of view of developing new PHB materials. The Mg,Al–TSPP LDH intercalation compound was obtained by anion exchange using a Mg,Al–LDH precursor in the chloride form, after soaking at 60°C for 1 week. The measured basal spacing increased from 8.0 Å for the chloride LDH to 22.4 Å for the TSPP form, i.e. a gallery height of 17.6 Å, fairly close to the side of the almost perfect square molecule of TSPP (18 Å). From X-ray diffraction and chemical analysis it was concluded, however, that exchange was not complete and that ca. 15% of the anion exchange capacity of the anionic clay corresponded to intercalated carbonate. Basal spacing, molecular size, and layer charge density suggested thus that the intercalated porphyrin anions were arranged with the molecular plane perpendicular to the brucite-like layers, Fig. 6.

Intercalation of *meso*-tetrakis(*p*-carboxyphenyl)porphyrin (hereafter pTCPP) [88] in Zn,Al–LDH, and of the atropoisomer ($\alpha\alpha\alpha\alpha$) of *meso*-tetrakis(*o*-carboxyphenyl)porphyrin (oTCPP) and the ammonium salt of the *meso*-tetrakis(*p*-sulfonatophenyl)porphyrin (pTSPP) [89] has been reported by Besse et al. Intercalation was conducted by coprecipitation at constant pH or anion exchange of a Zn,Al–LDH in the chloride form, leading in both cases to pure LDH phases, while by the calcination (300°C for 18 h)–reconstruction method significant amounts of ZnO were found. The diffraction patterns are characteristic of a structural disorganization, probably arising from a turbostatic effect induced by both the highly separated sheets, and the weak bond interactions between the interlayer species and the host lattice. Also, crystallinity is lower than for the chloride LDH, although it was improved by hydrothermal treatment at autogenous pressure.

Pure LDHs were obtained only for Zn/Al ratios of 2 and 3; larger values lead to coprecipitation of ZnO, while lower values lead to formation of amorphous aluminum hydroxide. Basal spacings ranged randomly (i.e. with no relation to the Zn/Al ratio) from 22.24 to 23.09 Å, probably because of different hydration degrees. However, the *a* dimension of the unit cell (equivalent to the average distance between two closest metal cations in the brucite-like layers [3]) steadily increased from 3.02 to 3.10 Å for the samples prepared by coprecipitation, as the

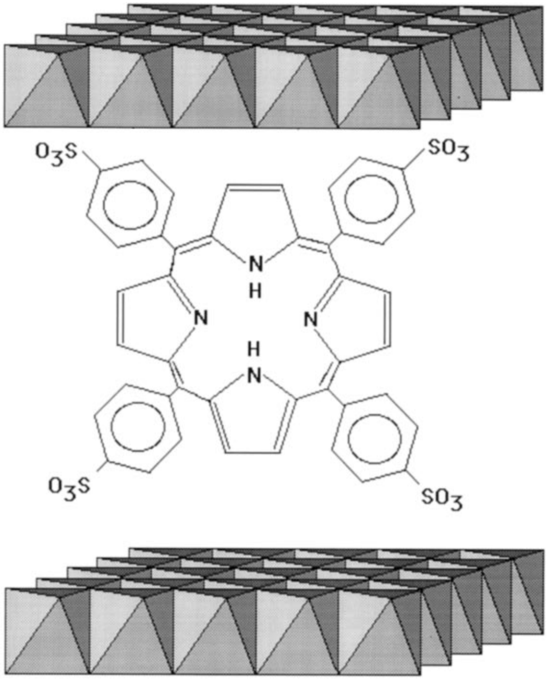

Fig. 6. Proposed orientation of 5,10,15,20-tetra-(4-sulfonatophenyl)porphyrin (TSPP) in the interlayer space of a Mg,Al layered double hydroxide. Adapted from Ref. [86].

Zn/Al ratio was increased. From the basal spacings and the size of the intercalated anions [90], these authors conclude [88,89] that the anion (pTCPP and pTSPP) should be located in a perpendicular orientation relatively to the layers, with the four anionic groups in tight interactions with the hydroxylated sheets, in a fashion similar to that above described for the Mg,Al–TSPP LDH [86] material. Such an arrangement would also be consistent with the layer charge density, that corresponds to 33 Å^2 per unit charge for the sample with a Zn/Al ratio of 3; an arrangement of the interlayer anion in horizontal position would correspond to 49 Å^2 per unit charge, while in the vertical position it corresponds to 15 Å^2 per unit charge. On the contrary, although the basal spacing measured for the LDH–oTCPP compound (18.5 Å) could be fitted also with a vertical disposition (this molecule is ca. 3.2 Å smaller than the other two), such an arrangement would decrease the hydrogen bonding interaction between the carboxylate groups and the hydroxyl anions in the brucite-like layers. Consequently, a parallel disposition of two molecules has been claimed in this case [89].

The photochemical properties of this sort of macromolecules can be modified when located in the interlayer space of an LDH. Tagaya et al. [91] have studied the intercalation of colored organic anions (pTSPP and pTCPP) in Mg,Al and Zn,Al LDHs by the reconstruction method. As in the cases above described [86,88,89], the basal space increase is consistent with a vertical orientation of the anions (spacings up to 30.7 Å, depending on the nature of the porphyrin), although the guest/host ratio varied from 48 to 100%. The absorption maxima of these colored organic anions are solvent-dependent, although no clear correlation exists between the wavelengths of the absorption maxima and the dielectric constant of the solvents [91]. When intercalated, a shift towards the red was observed for both anions, which has been explained on the basis of a close packing of anion molecules in the interlayer space, an effect similar to that previously reported for methylene blue adsorbed on a clay [92].

Incorporation of metal cations coordinated by macroligands in the interlayer space of LDHs has also deserved very much attention. In the case of the Zn,Al–pTCPP system, complexation of copper in the interlayer nanospace was attained simply by suspending the organic-LDH solid in a solution of copper nitrate [88], and metallation was confirmed by UV–vis and EXAFS spectra. In the UV–vis region, metallation leads to a slight red-shifting of the Soret band recorded at 400–450 nm for the free anion, while only two Q bands are recorded between 500 and 650 nm, and these results were observed for the Zn,Al–pTCPP–Cu(II) system. From EXAFS spectra, radial distributions around the Cu(II) were similar for $Cu(NH_3)_4SO_4 \cdot H_2O$ (with four equatorial nitrogen atoms and two oxygen atoms from water molecules in *trans* geometry) and for Cu(II)–pTCPP, with four nitrogen atoms in a planar environment around the copper cation at ca. 2.10 Å and Cu–Cu interactions along the direction perpendicular to the chelating ligand. For the Zn,Al–pTCPP–Cu(II) system, the radial distribution reveals a nearly regular octahedral environment, probably due to completion of the copper coordination sphere by two water molecules, thus further confirming the perpendicular arrangement of the porphyrin pillars in the interlayer space, as well as the absence of Cu–Cu interactions.

Intercalation of tetracarboxyphthalocyanine cobalt (II), TPC–C, in Zn,Al and Mg,Al–LDHs was carried out by the reconstruction method by Tagaya et al. [91]. The guest/host ratio was 100% for the Zn,Al system, with a basal spacing of 24.8 Å, i.e. the plane of the guest anion perpendicular to the plane of the host layers. However, for the Mg,Al system the basal spacing was 7.9 Å. Although these authors claim this value being consistent with a small amount (not quantified) of intercalated TPC–C, this basal spacing coincides with the value reported in the literature for carbonate containing Mg,Al–LDHs [3], and so it is possible that no intercalation of the macrocyclic was attained.

Complexes with macrocyclic ligands can be also incorporated in the interlayer space of LDHs via anionic exchange. Dutta and Puri [39] have reported complete ion exchange of nickel(II) phtalocyaninetetrasulfonate ion in the Al_2Li–LDH in the chloride form. Quite surprisingly, the basal spacing was 10.61 Å, a value quite close to that reported for phosphate and sulphate-containing LDHs, indicating that the phtalocyanines are parallel (‘flat’) to the aluminate layer and not arranged in a stacked fashion, which would require a spacing close to 22 Å.

Cobalt(II) phtalocyanines, specifically Co(II) phtalocyanine-3,4′,4″,4‴-tetrasulfonate (hereafter CoPcTs) have been also introduced in the galleries of Mg,Al LDHs by reconstruction of the hydrotalcite precursor calcined at 500°C and exposed to excess aqueous Pc salt at 60°C [76] or hydrothermally at 100°C [93], the solid displaying a basal spacing of 23.3–23.7 Å, Fig. 7. This is in agreement with a tilted orientation with respect to the hydroxide layers, with the axis joining the non-coordinating nitrogen atoms of the CoPcTs molecule oriented almost perpendicular to the hydroxide layers. These Co(II)–PcTs-containing LDHs have been tested as catalysts for autoxidation of 1-decanethiol [76] and 2,6-di-*tert*-butylphenol [93,94] by Pinnavaia et al., who have concluded that the catalyst becomes extremely stabilized in the gallery space of the LDH, if compared to its stability under homogeneous catalysis conditions; deactivation of the LDH-supported catalysts during 1-decanethiol oxidation was not observed even after five catalytic cycles for a total of more than 770 turnovers, while the homogeneous catalyst was deactivated after 25 turnovers; such a stabilization was even greater during 2,6-di-*tert*-butylphenol oxidation (3200 vs. 25 turnovers).

Carrado et al. [95] have synthetized Mg,Al LDHs intercalated with CuPcTs by hydrolysis of mixed aqueous salt solutions in the presence of NaOH, a method previously proposed by Park et al. [96], who first reported the direct synthesis of organic dyes into LDHs. Anionic exchange was achieved only when starting from a freshly prepared slurry (‘wet’ anionic exchange) of the LDHs (in the nitrate form), exchanged under carbon dioxide-free conditions, and an aqueous CuPcTs solution; however, no satisfactory products were obtained when the exchange was performed with dry LDH (also in the nitrate form) redispersed in water. Basal spacing for

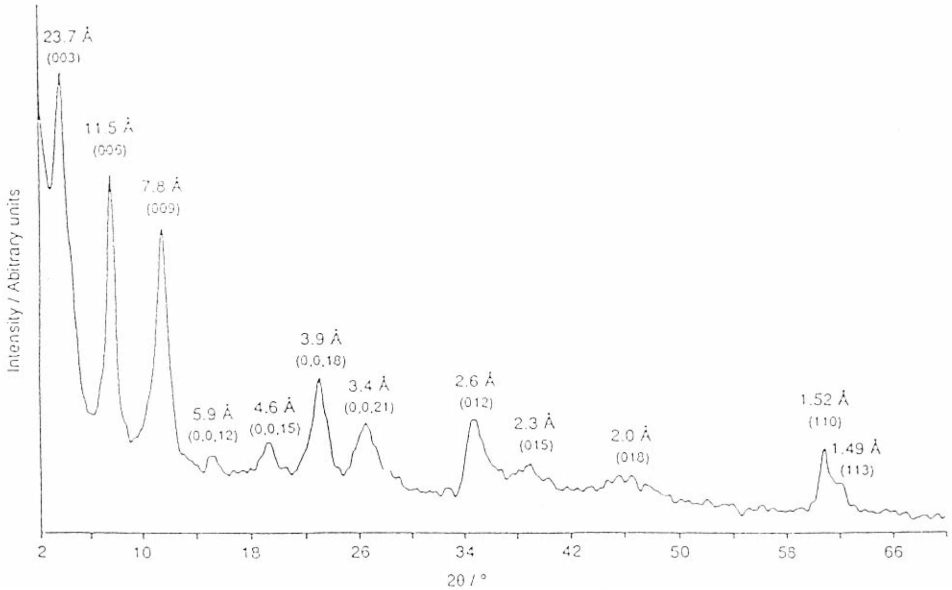

Fig. 7. X-ray diffraction pattern (Cu–K_α) of an oriented film sample of Mg,Al–[Co(PcTs)] LDH. Reprinted from M. Chibwe, T.J. Pinnavaia, Stabilization of a cobalt(II) phtalocyanine oxidation catalyst by intercalation in a layered double hydroxide host, J. Chem. Soc. Chem. Commun. (1993) 278–280, © 1993, with permission from The Royal Society of Chemistry.

both samples (prepared by direct synthesis and by anionic exchange) was 22.5–23.0 Å, but crystallinity was better for the sample prepared by wet anionic exchange. This spacing is markedly larger than that obtained (14–16 Å) for hectorite interlayered with cationic copper(II)-containing dyes, such as alcian blue. The difference arises from the different layer charge density for these cationic and anionic clays. The anionic clay prepared by these authors had a layer charge density close to 34 Å^2 charge^{-1}, a value only reached by micas among the cationic clays. From elemental chemical analysis and molecular modelling, and taking into account the layer density charge, Carrado et al. have concluded [95] that the phtalocyanine molecules are oriented in a tilted arrangement, in agreement with similar previous results by Pinnavaia et al. [76,93]. On the contrary, in the case of the hectorite clays, their lower layer charge density leads to a flat orientation of the phtalocyanine anions.

In addition to the increased stability (probably because the immobilization process inhibits the deactivating dimerization and self-oxidation reactions occurring in the homogeneous catalyst), it should be noted the large reactivity of the heterogeneous Co(PcTs)–LDH catalyst, despite the extremely low specific surface area, 28 m^2 g^{-1}, as determined from nitrogen adsorption, i.e. the nitrogen molecules are merely adsorbed on the external surface of the crystallites, without accessing the gallery space. So, 2,6-di-*tert*-butylphenol, with a much larger Van der Waals radii, does not access either, and thus only the Co(II) ions held at crystallite edge sites and external basal surface sites are able of participating in the oxidation reaction. This conclusion is supported by the finding that a similar system, but with a lower charge layer density (with Mg/Al ratio of 4, instead of 2), and thus with a greater separation between the intercalated cobalt centers, shows a 5-fold increase in activity.

This same cobalt phtalocyaninetetrasulphonate has been incorporated into a Zn,Al LDH by coprecipitation at constant pH from a Zn and Al nitrates solution and the Co complex. The solid isolated showed an interlamellar spacing of 23.0 Å, in close agreement with data previously reported [76]. This compound has been used for in situ studies of cyclohexene oxidation by combined EXAFS/XRD techniques studies [97].

Similar compounds containing increasing amounts (2–90 μmol g^{-1} of LDH support) of Co(II) phtalocyanine tetracarboxylate or Co(II) phtalocyanine tetrasulfonate have been tested by Iliev et al. for 2-mercaptoethanol oxidation [98]. Incorporation of the complexes into the interlayer space was achieved in this case by soaking the LDH (previously calcined at 450°C for 24 h in argon) with a solution of the sodium salts of the phtalocyanines, at 60°C for 7 days in argon. However, while the basal spacing was close to 22.7 Å in both series of samples (in agreement with the values reported by the authors previously cited), in the case of the carboxylate phtalocyanine, crystallization of its sodium salt, most likely on the external surface of the LDH crystallites, was also observed. The ESR spectra of these samples showed, for low Co and Cu(II) phtalocyanine concentrations (5 μmol g^{-1} of LDH support), a hyperfine splitting from ^{57}Co ($I = 7/2$) and from ^{63,65}Cu ($I = 3/2$), together with superhyperfine splitting from ^{14}N ($I = 1$) in the case of the

Cu(II)-containing sample. These results are consistent with magnetically distributed complexes in these low-concentrated samples. In addition, when the complex concentration was raised to 60 μmol g^{-1} of LDH support, spectra characteristic of aggregated and microcrystalline complexes were also recorded, specially a narrow singlet at $g = 2.004$, specific of the sodium salt of Co(II) phtalocyanine tetracarboxylate crystallites having deffects in the crystal lattice [99–101]. This signal did not disappear even after repeated heating–evacuation–purging cycles, thus meaning that the singlet is not due to superoxo complexes formed by the monomeric Co(II) phtalocyanine molecules.

The catalytic effectiveness of the Co(II) containing LDHs for 2-mercaptoethanol oxidation (to the disulfide) decreases as the concentration of the complexes is increased, a fact probably related to aggregation and crystallization of the phtalocyanine complexes, similarly to previous results for thiol oxidation using cobalt complexes anchored on ion exchange resins or other supports [99,102,103]. The turnover frequency was higher when water:DMF (1:3) was used instead of water as solvent for the Co(II) phtalocyanine complex during preparation of the compounds. Moreover, it is well known [104] that μ-peroxo complexes between neighboring ion exchanged molecules are low active for this catalytic reaction, and a similar effect would possibly account for differences found in the series of compounds studied by Iliev et al. [98]; this would nicely explain the small differences found by these authors when using water or water:DMF as solvent for preparing the samples, as the water:DMF mixture would permit a better molecular dispersion of the complex in the hydrotalcite host.

Further evidences of the effect of layer charge density on the orientation of the hosted phtalocyanine and porphyrine complexes has been obtained from UV–vis and ESR studies of these complexes intercalated in hectorite, fluorhectorite and a hydrotalcite-like LDH, three layered materials with markedly different charge layer densities [105]; it has been also found that the hydration state of the galleries modifies the orientation of the hosted anions. So, Co(II) tetrakis(*N*-methyl-4-pyridiniumyl)porphyrin (CoTMPyP) was intercalated in low layer charge density (80 $Å^2$ $charge^{-1}$) hectorite and in large layer charge density (27 $Å^2$ $charge^{-1}$) fluorhectorite by reacting the clay with an aqueous solution of the complex, under nitrogen, and different loadings were achieved. Co(II) tetrasulphophthalocyanine (CoPcTs) anion was intercalated in Mg,Al LDH (layer charge density 25 $Å^2$ $charge^{-1}$ [106]) following a method similar to that described by Pinnavaia et al. [76,93]. The basal spacing for the hectorite intercalate was 14.05 Å, changing to 14.00 Å after dehydration and outgassing in vacuum; thus, the complex plane should be very likely lying parallel to the clay layers. The basal spacing was slightly lower (12.6–13.8 Å) for the low loaded complex-clay systems, values similar to those reported for montmorillonite-hosted CoTMPyP [80]; such a basal spacing decrease at low loadings of large cations is commonly observed for smectite clays and attributed to irregular stratification and/or domain formation in the interlayers [107]. For the fluorhectorite compound, the basal spacing was 19.6 Å, decreasing to 17.6 Å upon dehydration. These values are consistent with either a face-to-face bilayer or a monolayer with the porphyrin being tilted at an angle (35° has been

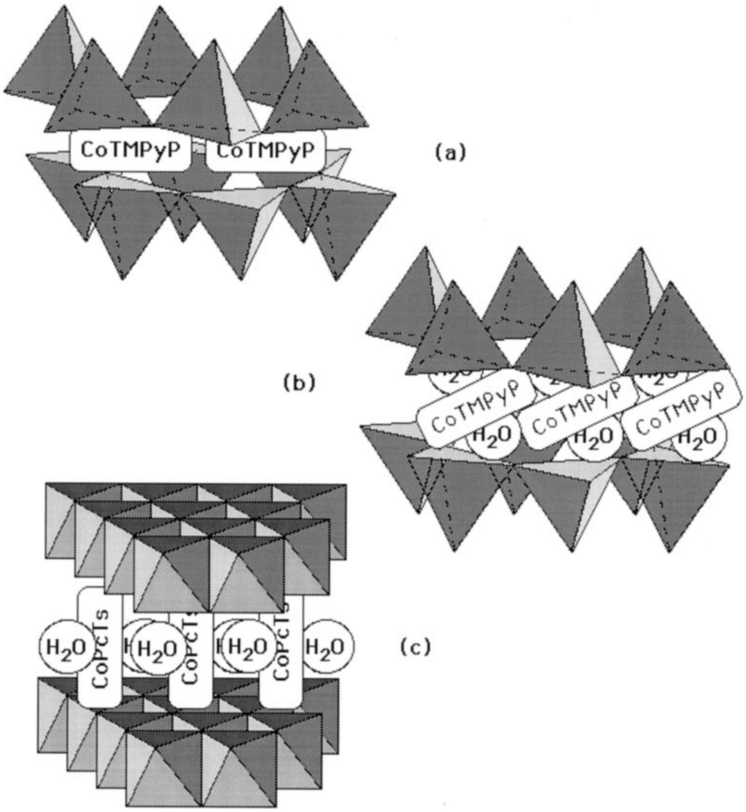

Fig. 8. Arrangement of Co(II)-tetrakis(*N*-methyl-4-pyridinium)porphyrin (CoTMPyP) in (a) hectorite and (b) fluorhectorite, and (c) of cobalt(II) tetraulfophtlalocyanine (CoPcTs) in a layered double hydroxide. Adapted from Ref. [110].

calculated [108]) to the clay layers. Finally, the basal spacing was 23.5 Å, and did not change upon dehydration, for the LDH-hosted CoPcTs, a value similar to that reported by these and other authors [76,93,95,98], Fig. 8.

While the UV–vis spectra of the hectorite and fluorhectorite systems do not change sensibly upon exposure to O_2 (suggesting that intercalated Co macrocycles do not form adducts with O_2, as observed in solution [109]), small changes in the positions of the Soret and Q bands for the CoPcTs–LDH compound have been related to changes in the electron density of the conjugated π orbitals of the macrocycle ring caused by confinement in the interlamellar space of the LDH, by interactions between neighboring CoPcTs and by changes in the inductive effect of the sulfonate groups.

ESR results are consistent with the XRD results, for the CoTMPyP–fluorhectorite compound in the hydrated state, if the molecular plane is tilted 27° with respect to the clay layers, and with one or two water molecules coordinating to the Co(II) along the z-axis. Upon dehydration, water molecules are removed, and the hosted molecules form a bi-layer, with the molecular plane oriented parallel to the clay layers, a similar disposition as that concluded for CoTMPyP–hectorite, although in this case only a monolayer of hosted molecules is formed, without coordinating water molecules. The orientation of CoPcTs in the LDH gallery could not be concluded from anisotropic ESR measurements, as no oriented films could be obtained. From XRD measurements, similar conclusions to those by Carrado et al. [95] were achieved, i.e. a perpendicular arrangement of the complex in the LDH gallery; similar spacing values could be explained by a non-favorable trilayer arrangement of the anions parallel to the LDH plane, but in this case the charge layer density would not be matched, and the spacing would be expected to decrease upon dehydration, but this was not observed. The ESR spectrum of CoPcTs–LDH was similar to that of air-dried CoTMPyP–hectorite, so further confirming the slightly tilted ‘upright’ orientation; however, it changes dramatically upon vacuum dehydration, with a weak ESR signal at $g \approx 2$, probably because aggregation of the hosted molecules upon water removal; this process is reversible upon rehydration and water diffusion into the interlayers.

From these results, these authors conclude [105] on the suitability of the fluorhectorite and LDH compounds, but not the hectorite-hosted one, for catalytic reactions taking place on the Co(II) sites, accesible to reactant molecules for electron-transfer reactions, behaving as biomimetic catalysts, as observed for 2,6-di-*tert*-butylphenol oxidation [94].

These three host–guest systems have been also tested for reductive dechlorination of carbon tetrachloride [110], and the results compared with those obtained for the same Co compounds in homogeneous conditions, and by silica-supported CoTMPyP. While under homogeneous conditions, both chloroform and dichloromethane were formed, only the former was observed under heterogeneous conditions, accounting for less than 30% of degradated CCl_4, which is consistent with previous studies of degradation by Co macrocycles [111–115]. Degradation of CCl_4 follows a first-order kinetics. Under homogeneous conditions, the initial rate rapidly decreases, indicating deactivation of the catalyst, probably because aggregation in aqueous solution [116], but as aggregation is hindered in the clays gallery, activity is maintained. The lack of formation of dimethylmethane has been attributed [110] to a change in the reduction potential of the supported macrocycle because of the charged layers. Initial rate constants for heterogeneous CCl_4 degradation (as calculated along the first 30 min of reaction) decreases when using the supports silica-gel > LDH > fluorhectorite > hectorite. This decrease is in agreement with accessibility of the reactant molecules to the Co(II) sites, as concluded from XRD and ESR studies [94,105] for the layered materials. Overall, the dechlorination reaction in these heterogeneous systems is very similar to enzyme-catalyzed reactions, and the initial degradation rate (R_0) can be fitted by the Michaelis-Menten kinetic model:

$$R_0 = v_{max}[CCl_4]_0/([CCl_4]_0 + K_m) \tag{6}$$

where v_{max} is the maximum reaction rate for a specified initial Co macrocycle concentration and K_m is the Michaelis constant. v_{max} values decrease for the catalysts supported on silica-gel > LDH > fluorhectorite > hectorite, i.e. as the initial reaction rate does, and in agreement with studies on the orientation and hydration of the macrocycles in the interlayers [105].

Zikmund et al. have recently proposed an alternative route to the synthesis of LDH-hosted coordinatively unsaturated Co(II) complexes, consisting in the in situ synthesis of the complex inside the LDH gallery [117]. The route is rather different to those described above. First of all, these authors prepare the Mg,Al–carbonate LDH by reaction of solid magnesium carbonate hydrate with an aqueous solution of sodium aluminate and sodium hydroxide. After calcination at 500°C in air for 5 h of the washed solid, it was suspended in carbon dioxide-free distilled water, leading to the reconstructed OH-containing LDH (meixnerite). Exchange of the interlayer hydroxyl groups by amminocarboxylates (L-glutamate and isonicotinate) was achieved in a glycol:water (2:1) mixture, to facilitate swelling of the solid. Suspension of this solid in an ethylene glycol solution of $CoCl_4^{2-}$ led to scavenging of Co ions in the galleries in the form of ion pair species, and hopefully intercalated $CoCl_3$–glutamate (or $CoCl_3$–isonicotinate) species. Mixing with Schiff bases salen or salophen under argon led to intercalated coordinatively unsaturated square planar Co(II) chelates. The d–d diffuse reflectance spectra of these compounds were similar to those of the analogous complexes in solution and in Y-zeolite cages. Their basal spacings were 13.1 and 11.6 Å, respectively, for the salen and salophen derivatives, thus suggesting the anions have their molecular plane parallel to the LDH layers. When air was contacted with the Co(salen) or Co(salophen) derivatives, the ESR spectrum showed two signals: a narrow one (signal I) with $\delta H = 120$ mT showing hyperfine structure, and a second signal (II) with $g = 2.02$ and $\delta H = 950$ mT. On heating at 300°C, signal II is removed, but it is restored after decreasing the temperature. This oxygenation–deoxygenation process was undefinitely reversible. As no ^{59}Co hyperfine splitting was observed in signal I, it was attributed to superoxide species interacting with Al^{3+} ions, while signal II strongly resembles that observed for other immobilized Co(salen)–dioxygen complexes.

Macrocyclic complexes of other first-series transitions cations have been also exchanged into the interlayer space of LDHs. Mansuy et al. [75] have reported the preparation and catalytic properties of Mn(III) porphyrins (TSPP, dianion of *meso*-tetrakis-(4-sulfonatophenyl)porphyrin, and TDCSPP, dianion of *meso*-tetrakis-(2,6-dichloro-3-sulfonato-phenyl)porphyrin) supported on LDHs and other supports, for alkane and alkene oxidation. The complexes were hosted via the reconstruction method of previously calcined (450°C) Mg,Al–LDH in its carbonate form; the complex was not released in the presence of organic solvents (e.g. dichloromethane, methyl cyanide, methanol), and its UV–vis spectra showed the expected Soret band for Mn(III) porphyrins. Upon comparison with these same Mn(III) porphyrins supported on alumina, the LDH-supported one showed a rather low catalytic activity for heptane hydroxylation, but it gave the highest regioselectivity for hydroxylation at the terminal positions. Manganese porphyrins intercalated-LDHs have been also studied as electrode modifiers [118].

A rather complex system containing LDHs has been described by Robins and Dutta for photochemical processes [119]. These authors have prepared a LDH photochemical assembly consisting of a Li,Al–LDH hosting titanium dioxide and myristate anions, together with [tetrakis-(4-carboxyphenyl)porphyrinato] zinc(II), (ZnTPPC). First, the Li,Al–LDH anionic clay interlayered with myristate ($CH_3(CH_2)_{12}COO^-$) was prepared; the interlayer spacing was 21 Å, consistent with a monolayer of anions in all-*trans* configuration. Upon treatment with an hexane solution of titanium butoxide the interlayer spacing increased to ca. 25 Å, and the XRD peaks became slightly broader; controlled hydrolysis led to interlayer TiO_2 particles, the diffraction peaks sharpening up somewhat and with similar spacings as to the original Li,Al–myristate. Finally, incorporation of Zn(TPPC) was achieved by partial anionic exchange of the myristate anions; the diffraction pattern was similar as for the Li,Al–myristate material, but, considering that the porphyrin dimension is ca. 18 Å (smaller than the spacing measured for the myristate LDH), the porphyrin molecule could be held with its plane perpendicular to the metal-hydroxide layer, as previously reported [76,95,105] for phtalocyanines in Mg,Al LDHs. The emission spectra of the solid (excitation wavelength 406.7 nm) resembles that of Zn(TPPC) in water and ethanol, where no aggregation of the porphyrin molecules exists [120,121], suggesting the complex is dispersed, and not forming aggregates in the interlayer space of the LDH. The Soret band broadens and slightly shifts from 425 to 420 nm, but this changes cannot be due to aggregation (as concluded from the emission spectra results), and so should be due to interaction in the interlayers, probably by hydrogen bonding to the framework hydroxyl groups, and costrained orientation of the benzoic acid rings, in a similar fashion as that described by Pinnavaia et al. [105] for clay-hosted cationic porphyrins. Further shift to 410 nm is observed upon incorporation of TiO_2, probably because hydrogen bonding, as also concluded from Raman spectroscopy measurements.

This intercalated porphyrin promotes viologen (heptyl viologen and propyl viologen sulfonate, PVS) reduction upon excitation, in the presence of EDTA as sacrificial electron donor, Fig. 9. This scheme implies that the photochemical reaction takes place near the edge of the LDH particle, quite reasonably, as TiO_2 is formed by hydrolysis of titanium tetrabutoxide by ambient moisture, and water is not expected to penetrate deep into the LDH, that had become rather hydrophobic upon exchange with myristate anions.

3. Systems hosting oxometalates

Polyoxometalates with several nuclearities have been incorporated into the interlayer space of different LDHs. These studies have been carried out on LDHs with a wide variety of cations in the layers, but, in relation to the nature of the intercalated anion, it is limited by the chemistry of metal ions forming oxometalates. Derivatives of chromium and vanadadium are those most widely studied, although several reports have been also published on molybdenum and manganese compounds. On the other hand, the number of papers published on systems containing iso- and hetero-polyanions with a Keggin-like or related structure, is rapidly increasing in recent years. General reports on the preparation of polyoxometalates–intercalated LDHs and their applications have been published [84,122–124]. In this section, classification has been made according to the nuclearity and nature of the interlayer anion.

3.1. Layered double hydroxides intercalated with low-nuclearity oxometalates

The reactivity of simple oxometalates, such as chromate and dichromate, inside interlamellar domains of Zn,Al or Zn,Cr, or Cu,Cr–LDHs after ageing under moderate thermal treatment, has been studied. Pillaring and grafting processes have been put into evidence from structural and spectroscopic data for these compounds, and their application in several catalytic processes has been also tested.

Layered double hydroxides hosting intercalated CrO_4^{2-} have been prepared by Miyata and Okada [72] by coprecipitation (direct synthesis). The bright-yellow solid prepared, Mg,Al–CrO_4^{2-}, contains, however, ca. 2% intercalated carbonate, incorporated during the synthesis or drying step. As already mentioned, total exclusion of carbonate is rather difficult to achieve, especially when metals forming highly basic hydroxides (e.g. Mg^{2+}) are used. Consequently, the ratio between the total negative charge provided by interlayer anions (carbonate and chromate) and total positive charge in the layers (due to aluminum) was 1.13, instead of the expected value of 1.0, suggesting that the excess anions are strongly adsorbed on the positively charge surfaces. The XRD spacing for planes (003) was 8.94 Å, corresponding to an interlayer space of 4.06 Å. This value is lower than that reported by Miyata et al. [125] for an LDH intercalated with perchlorate (interlayer space 4.38 Å), despite the size of CrO_4^{2-} and ClO_{4-} are almost the same; the difference has

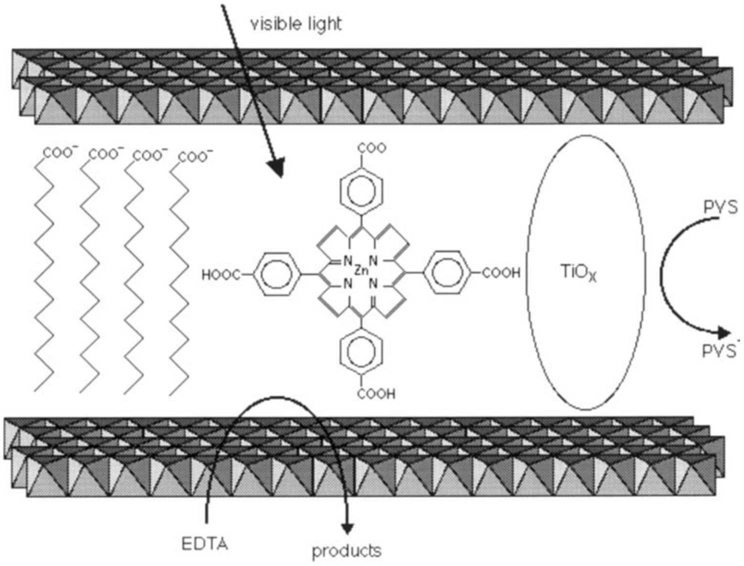

Fig. 9. Scheme of a layered double hydroxide photochemical assembly. Adapted from Ref. [119].

been attributed by these authors [72] to a stronger interaction of the divalent chromate anions than of the monovalent chlorate anions with the layers. The IR spectrum band ν_1 of chromate, IR forbidden for a pure T_d symmetry, is recorded at 865 cm^{-1}, while band ν_3 splits into three absorptions at 845, 885, and 950 cm^{-1}, confirming a symmetry close to C_{2v} for the CrO_4^{2-} anion in the interlayer space of the LDH. On calcination, removal of interlayer water up to 350°C gives rise to a small decrease in $d(003)$, but at 400°C the layered structure collapses, forming MgO, and above 800°C the spinel $MgAl_{2-x}Cr_xO_4$ is detected.

The reconstruction method, from a Mg,Al–LDH calcined at 450°C, has been applied by Chibwe and Jones [32] to intercalate $Cr_2O_7^{2-}$ by suspending the powder in a decarbonated solution of $K_2Cr_2O_7$. No interference of carbonate is reported, and the interlayer space was 10 Å, with the C_2 axis of the guest species oriented perpendicular to the brucite layers. However, a value of 8.4 Å has been reported by Misra and Perrotta [126] for a Mg,Al–LDH prepared following the same method, but using $Na_2Cr_2O_7$ instead of the potassium salt, as the precursor; this value is fairly close to that reported by Miyata and Okada [72] for intercalation of chromate, and so it is possible that dedimerization of the dichromate has taken place during synthesis.

A similar, although slightly lower, value of 8.25 Å has been reported by Besse et al. [127] for a Cu,Cr–LDH intercalated with CrO_4^{2-}. Layered double hydroxides containing Cu or Zn in the brucite like layers are not usually prepared by the conventional methods described in the literature [2,3] because their hydroxides do not possess the brucite-type structure; instead, they are prepared by adding an aqueous solution of a salt of the trivalent cation (Cr(III) chloride in this case) to a suspension of the oxide of the divalent cation (CuO), and further Cl^-/CrO_4^{2-} anionic exchange (No pH control is mentioned by Besse et al. [127]). The thermal properties of this compound are worthwhile to be analyzed in detail. Upon calcination at 300°C, the weight loss recorded is attributed to dehydration (removal of interlayer water molecules) and also dehydroxylation (from the brucite-like layers), the layered structure collapsing, and forming $CuCr_2O_4$ and CuO at 520°C. This behavior is rather similar to that observed for other LDHs. However, when the calcination is performed at 80°C, the interlayer spacing decreases from 8.25 to 7.32 Å, while only a small decrease (due to dehydration) is observed for the chloride analogous in the same temperature range. For the chromate compound, the decrease in spacing is not consistent with dehydration only, taking also into account that the size of the chromate tetrahedron is larger than that of the chloride anion, and so these authors suggest some bonding (grafting) between chromate and the layer. This was confirmed after observing that despite CrO_4^{2-}/Cl^- exchange is observed for the uncalcined Cu,Cr–CrO_4^{2-}, such an exchange is not observed after calcination at 80°C.

Grafting has been also observed for the dichromate analogous [128] prepared by ionic exchange at pH 4.5 (the chromate compound is obtained at pH 8.5). EXAFS and XANES studies [129] show that the local environment of the copper cations is not affected by the exchange, and consists of a strongly tetragonal elongated distorted octahedron. Storing conditions of the exchanged materials are important

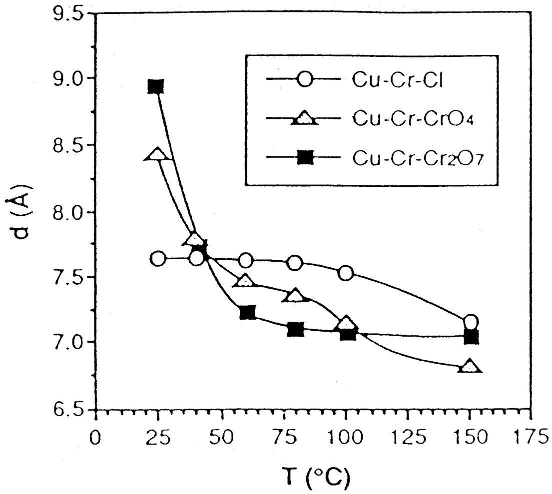

Fig. 10. Effect of heating on interlayer spacings of Cu,Cr–X LDHs (X = Cl^-, CrO_4^{2-}, $Cr_2O_7^{2-}$). Reprinted from C. Depège, C. Forano, A. de Roy, J.P. Besse, [Cu–Cr] layered double hydroxides pillared by CrO_4^{2-} and $Cr_2O_4^{2-}$, Mol. Cryst. Liq. Cryst. 244 (1994) 161–166, © 1994, with permission from Gordon & Breach Science Publishers SA.

in determining the interlayer space, due to the ability to adsorb water in the interlayer space, as confirmed by thermogravimetric and elemental chemical analyses. The spacings determined from X-ray diffraction were 8.95 Å and 8.42 Å, respectively, for the dichromate and chromate compounds, these values being markedly lower than those reported by Chibwe and Jones [32] for a Mg,Al–$Cr_2O_7^{2-}$ LDH. These values, however, are close to that reported by Miyata and Okada [72] for the chromate form, and so a dedimerization could happen. Both phases undergo a slow evolution to contracted forms with basal spacings of 7.68 Å (chromate) and 7.87 Å (dichromate) upon water removal, Fig. 10, and these extremely low values cannot account for free oxoanions, but evidence an effective pillaring on the hydroxylated sheets. The difference with the behavior observed with other chromate-containing LDHs has been attributed [128] to the specific chemical properties of copper, which can form a wide range of lamellar copper hydroxides $Cu_2(OH)_3A$ (A = Cl^-, ClO_4^-, NO_3^-, MnO_4^-, etc.) [130] with short interlayer distances. However, such pillaring is reversible, as evidenced by the ability to exchange by chloride in the presence of an excess of KCl. A decrease in the basal spacing to 7.10 and 7.30 Å is observed for the chromate and dichromate forms, respectively, upon heating at 80°C [128], the decrease is not reversible, and the anions cannot be further exchanged, indicating that this rather soft treatment has been able to anchor the anions to the layers. Further heating at 200–300°C destroys the lamellar structure, as confirmed by X-ray diffraction and XAS measurements [129].

Similar spontaneous contraction of the layers has been also described for Zn,Al and Zn,Cr–LDHs intercalated with CrO_4^{2-} and/or $Cr_2O_7^{2-}$, but only after ageing or thermal treatment [131]. For Zn,Al–CrO_4 and Zn,Cr–Cr_2O_7 a decrease in the basal spacings from 8.61 to 7.86 Å and from 9.20 to 7.34 Å, respectively, is observed upon ageing the solid it its mother liquor, values too low to be compatible with free interlayer anions, despite they were easily exchanged for chloride. However, after treatment at 150°C for 24 h, exchange was not achieved, and the basal spacings decreased to values in the range 6.80–7.20 Å. From these and former studies [127,128], Besse et al. conclude that in the contracted phases formed prior to thermal treatment, also described as pre-grafted phases, the interlayer anions become close to the metal cations in the layers, by approaching one oxygen atom of the interlayer tetrahedron to one of the triangular voids of the hydroxide layers, so decreasing the interlayer space. On heating, as water molecules are removed, some of the hydroxyl groups are removed as well, effective anchoring of the anions taking place, Fig. 11.

Aldol condensation between formaldehyde and acetone to yield methylvinyl ketone has been studied by Suzuki and Ono [132] on several hydrotalcites calcined at 500°C. Although the most effective precursor was that containing Mg,Al–CO_3, a selectivity of 100% was reached upon CO_3^{2-}/CrO_4^{2-} exchange.

Oxidation of alcohols in non-polar media at r.t. has been achieved by permanganate anions intercalated in Mg,Al–LDH [133]. The reaction proceeds selectively to the corresponding aldehyde or carboxylic acid, depending on the starting

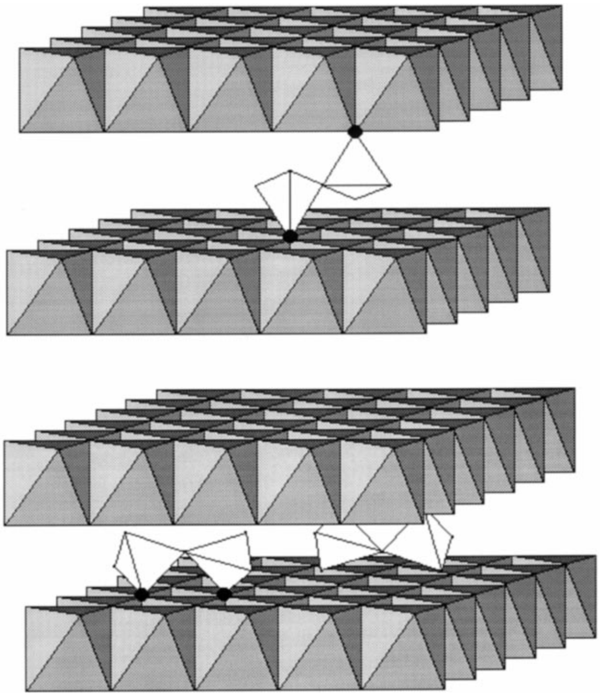

Fig. 11. Two ways of grafting of ditetrahedral anions ($Cr_2O_7^{2-}$, $V_2O_7^{2-}$) to layered double hydroxides.

alcohol. The selectivity towards benzaldehyde during oxidation of benzyl alcohol has been explained based on the low ability of the LDH to adsorb the aldehyde.

3.2. Layered double hydroxides intercalated with medium-nuclearity oxometalates: vanadates and molybdates

3.2.1. Vanadates

Among all metal-containing anions incorporated into the interlayer space of hydrotalcites and other LDHs, oxovanadates represent the widest studied group. Although mostly as decavanadate, some studies have been also devoted to intercalation of lower oligovanadates.

Oxometalate-pillared LDHs are in many cases prepared by a two-step anion exchange method, through intermediate intercalation of a large organic anion, to swell the brucite-like layers [65,134].

The polymerization degree of oxovanadates is pH-dependent, nuclearity increasing as pH decreases. For a 0.1 M aqueous vanadate solution, these equilibria are as follows:

$$V_{10}O_{26}(OH)_2^{-4},\quad V_{10}O_{27}(OH)^{5-},\quad V_{10}O_{28}^{6-},\quad \text{decavanadate},$$
$$\text{pH} = 1 - 3 \leftrightarrow$$
$$\leftrightarrow VO(OH)_3,\quad VO_2(OH),\quad V_3O_9^{3-},\quad V_4O_{12}^{4-},\quad \text{metavanadate},$$
$$\text{pH} = 4 - 6 \leftrightarrow$$
$$VO_3(OH)^{2-},\quad HV_2O_7^{3-}, V_2O_7^{4-},\quad \text{pyrovanade},\quad \text{pH} = 8 - 11 \leftrightarrow$$
$$\leftrightarrow VO_4^{3-},\quad \text{vanadate},\quad \text{pH} > 12.$$

In one of the pioneering works on LDH-intercalated vanadates, Twu and Dutta [135] prepared Li,Al–LDH with different oxovanadate oligomers by ion exchange of the Li,Al–Cl precursor with NH_4VO_3 aqueous solutions at different pH; it was expected anionic exchange and intercalation of the oxovanadate more stable at each pH. However, at pH larger than 13, selective Cl^-/OH^- exchange, but not chloride/vanadate, was observed. When the pH was lowered to 8–11, complete chloride/vanadate exchange was achieved, the basal spacing increasing from 7.8 to 10.8 Å. Although a compound with the same gallery height (6.0 Å, once the thickness of the brucite-like layer, 4.8 Å, is considered) is obtained after exchange at pH 5–6, the Raman spectra of both samples were completely different. Finally, at pH 3–4, only partial exchange was achieved, as a vanadate/chloride competition exists, because of the use of HCl to attain this low pH values. As different interlayer anions could give rise to the same gallery height (ca. 6 Å), thus making impossible to ascertain the actual nature of the interlayer anion, this was studied by Raman spectroscopy, based on results by Griffith et al. [136,137] for oxovanadate species. The most prominent Raman band of vanadate species, due to V–O stretching, occurs in the 800–1000 cm^{-1} range, shifting to higher wavenumbers as polymerization and/or branching increases. From this, it was concluded that at pH 10 the

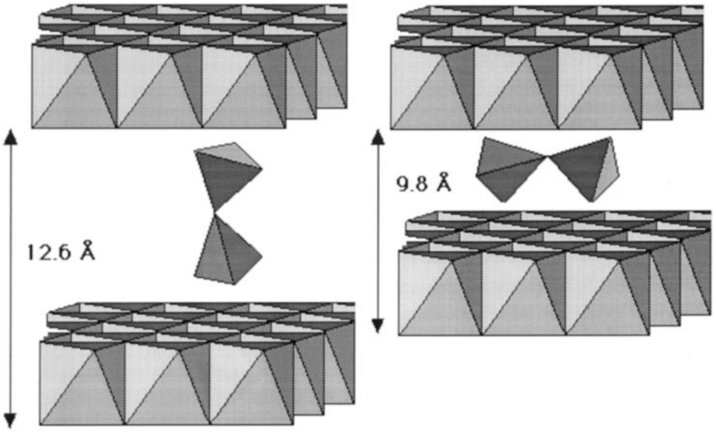

Fig. 12. Two possible orientations of $V_2O_7^{2-}$ in layered double hydroxides. Adapted from Ref. [135].

interlayer species is $V_2O_7^{4-}$ (also the major component of the solution at this pH), with the V–V axis parallel to the layers, Fig. 12(b), and also hosting interlayer water molecules; at pH 5–6 the interlayer species is $V_4O_{12}^{4-}$, with a similar gallery height, while at lower pH the predominant species still is $V_4O_{12}^{4-}$, with only a minor amount of $V_{10}O_{28}^{6-}$, despite the decavanadate can be completely exchanged in other hydrotalcites (see below).

On the other hand, the average charge per V atom changes from one oxovanadate to another. Taking into account that the negative charge of the interlayer anion should balance the positive charge of the Al-containing brucite-like layers, Bhattacharyya et al. [138] have prepared, through a careful control of pH during reaction and of the $NaVO_3/NaOH$ ratio in the starting solution (from 1:7 to 1:3), Mg,Al and Mg–Zn,Al–LDHs containing different oxovanadate oligomers by a single-step method. In all cases, an aqueous solution of the Mg and Al (or Mg, Zn, and Al) cations was dropwise added to the $NaVO_3/NaOH$ solution at the desired pH (10.8 for $V_2O_7^{4-}$ and 8.3 for $V_4O_{12}^{4-}$), the gelatinous mixture being heated for several hours at 80–90°C. The basal spacings determined by X-ray diffraction were 10.5 Å for the pyrovanadate, and 9.7 Å for the cyclotetravanadate.

The $V_2O_7^{4-}$ and $HV_2O_7^{3-}$ anions are constituted by two $[VO_4]$ tetrahedra sharing a vertex, and in the interlayer space, two different arrangements are possible [139], one with the V–V edge perpendicular to the brucite-like layers, with a calculated basal spacing of 12.6 Å (from the size of the $V_2O_7^{4-}$ anion derived from single crystal data for $Mg_2V_2O_7$ [140]), and another where it is parallel to the layers, with a calculated value of 9.8 Å, Fig. 12, a situation similar to that described by Chibwe and Jones [32] for intercalated $Cr_2O_7^{2-}$; in addition, the presence of water molecules can enlarge such a spacing. On the other hand, the smallest dimension of $V_4O_{12}^{4-}$ is expected to be the same as $V_2O_7^{4-}$ [138], and these authors conclude the anions should be in all cases in a ‘parallel’ disposition.

Similar studies have been carried out by Besse et al. [141] in a Cu,Cr–LDH, analyzing also the role of swelling agents to favor the exchange and incorporation of polyoxometalate species. At pH 10–11, $V_2O_7^{4-}$ is selectively exchanged, whereas as the pH is lowered, the major interlayer species are $V_2O_{12}^{4-}$ (pH 6–7) and $V_{10}O_{28}^{6-}$ (pH 4–5). These authors conclude that the size of the precursor anion used to swell the layers (terephtalate or dodecylsulphate), and hence the values of the interlayer distances, must favor the intercalation of vanadates of similar hinderance.

Delmas et al. [142,143] have recently proposed an alternative route, by the so-called 'chimie douce' (soft chemistry), to insert metavanadate in an LDH, Fig. 13. These authors claim the method overcomes the problem, usually found, that chemical composition of LDH shows fluctuations due to the different pH at which precipitation of $M(OH)_2$ and $M(OH)_3$ hydroxides occurs, thus leading to a chemical composition determined by the intrinsic stability of the solid, rather than by the composition of the starting solution. By high temperature synthesis methods these authors obtained a layered $NaNi_{1-y}Co_yO_2$ solid, with a layer–layer distance of 5.18 Å; an oxidizing hydrolysis with NaClO and KOH leads to an expansion to 7.08 Å and insertion of potassium ions, followed by reduction in H_2O_2/NH_4VO_3 solution. The asymmetry of the X-ray diffraction lines usually indexed as due to (101) and (111) planes, in some cases attributed to a turbostratic-like character (parallel and equidistant layers disoriented with regard to one another along the c-axis), has been attributed by these authors to local distortions within each layer, probably related to a misfit of the oxygen in the layers (O–O distance 3.04 Å) and in the metavanadate chains (2.91 Å). The interlayer spacing of the vanadium-con-

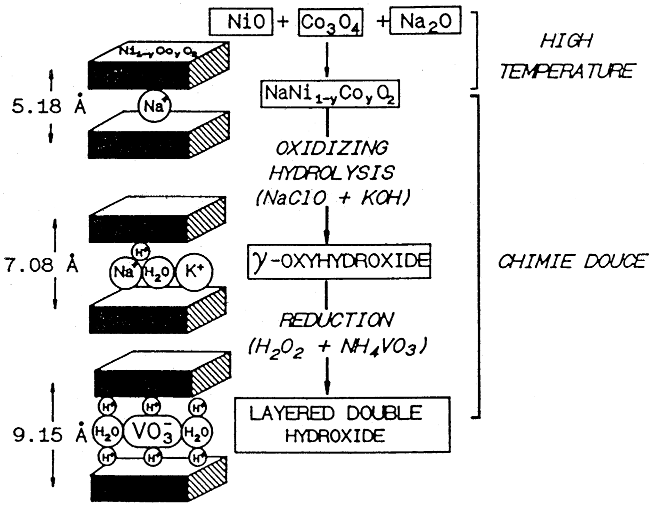

Fig. 13. Scheme showing the successive reaction steps involved in the preparation of a LDH by 'chimie douce'. Reprinted from K.S. Han, L. Guerlou-Demourgues, C. Delmas, A new metavanadate inserted layered double hydroxide prepared by 'chimie douce', Solid State Ionics 84 (1996) 227–238, © 1996, with permission from Elsevier Science.

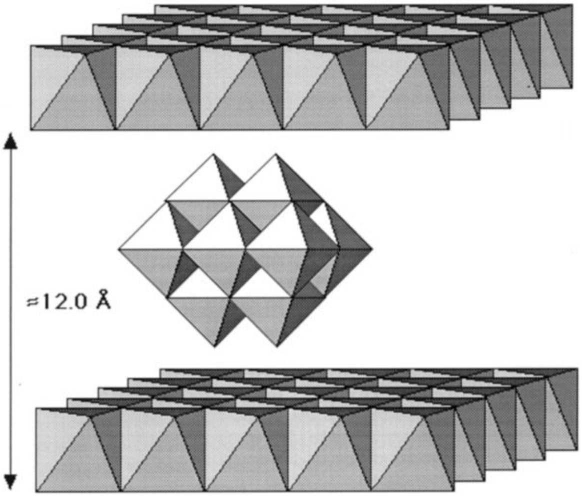

Fig. 14. Orientation of decavanadate anion, $V_{10}O_{28}^{6-}$, in the interlayer space of layered double hydroxides, with its 'main' C_2 axis parallel to the brucite-like layers.

taining material was 9.15 Å, and from IR data, the presence of polymeric, metavanadate species, $(VO_3)_n^{n-}$ (consisting of $[VO_4]$ groups with a C_{2v} symmetry) was concluded, in agreement also with chemical analysis, which suggest one negative charge per vanadium ion, while the presence of cyclic metavanadate entities, such as $V_3O_9^{3-}$ or $V_4O_{12}^{4-}$, was excluded.

Pinnavaia et al. have shown [134] that it is possible to introduce polyoxovanadate ions as pillars in LDHs containing Zn,Al or Zn,Cr or Ni,Al in the layers, in the chloride form. At pH 5.5–10 a byproduct containing $V_4O_{12}^{4-}$ was formed, but at pH 4.5 total exchange with $V_{10}O_{28}^{6-}$ was observed, with solids possessing a basal spacing of 11.9 Å, corresponding to a gallery height of 7.1 Å and a decavanadate orientation in which the C_2 axis is parallel to the host layers, Fig. 14. Retention of the structure of the interlayer anions was confirmed by ^{51}V MAS-NMR spectroscopy, while EXAFS studies at the Zn K-edge have shown [144] that no structural distortion occurs for the brucite-like host lattices upon intercalation, in agreement with electron microscopy studies which show that the exchange reactions are topotactic. Exchange from the nitrate form has been reported by Woltermann [145]. Photocatalytic oxidation of isopropyl alcohol to acetone was achieved on the Zn,Al–$V_{10}O_{28}$ LDH in the presence of oxygen, this catalyst being more active than the homogeneous catalyst, despite scattering of light by the host particles [134].

LDHs containing Zn and Al in the layers have been also prepared with interlayer vanadates, by ionic exchange of chloride or carbonate precursors [146]. It has been found that the Zn/Al ratio in the final Zn,Al–vanadate LDH decreases when the pH is lowered, probably due to selective dissolution of Zn^{2+}. Vanadium K-edge XAS data show that in samples prepared at low pH the major interlayer species is $V_{10}O_{28}^{6-}$, while as the pH is increased, interlayer vanadates consist of tetrahedral

$[VO_4]$ units, and it has been even possible to estimate the fraction of V^{5+} ions existing as decavanadate, tetravanadate or tetrahedra chains.

Drezdzon [65] has proposed an alternative method to prepare LDHs exchanged with large oxometalates, by intermediate preparation of organic-exchanged materials. It was expected that, since hydrotalcite-like materials have higher charge density than cationic clays, they would be more difficult to swell and exchange. A Mg,Al–terephthalate LDH was obtained from Mg and Al nitrates and terephthalate in basic (NaOH) medium, with a basal spacing of 14.4 Å (7.8 Å for the carbonate form). After addition of this solid to an aqueous NH_4VO_3 solution at pH 4.5, the basal spacing of the layered material obtained was 11.9 Å (coincident with the value reported by Pinnavaia et al. [134]). Acidification plays a double role: (i) polymerization of the metalate, and (ii) protonation of the organic anions, so making easy its removal from the interlayer space; however, it has been also claimed [147] that the process is inhibited by the poor solubility of the organic acid in water, and the resulting difficulty in its removal from the clay matrix.

A third method already mentioned to prepare other LDHs, different from exchange and pre-swelling with organic anions, was used by Jones et al. [148], from the known ability of calcined LDHs to recover the layered structure. An Mg–Al LDH calcined at 450°C for 18 h, suspended in an aqueous solution of $NaVO_3$, recovers the layered structure, hosting decavanadate species, as concluded from a basal spacing of 11.8 Å, after acidification with HCl at pH 4.5.

All these methods require the use of carbon dioxide-free conditions, in order to avoid incorporation of carbonate anions in the interlayer region. For acidic systems, such as the Zn,Cr–LDH system, Kooli and Jones have reported a direct method for the synthesis of decavanadate-containing Zn,Cr–LDH [149], at a pH where carbonate is not present in the solution. A solution containing Zn and Cr chlorides was added to an aqueous solution of $NaVO_3$ (pH 4.5), and the slurry obtained aged overnight at 55°C. The basal spacing for (003) planes was 11.89 Å, suggesting again an orientation of the decavanadate anion with the main C_2 axis parallel to the host layers. Expanded structures with interlayer $V_{10}O_{28}^{6-}$ anions were obtained for solutions with Zn/Cr ratios between 1 and 5, although the *a* parameter (related to the average cation–cation distance in the brucite-like layers, and hence, on the ionic radii of these cations and their nature and concentration) remains close to 3.11 Å, whichever the starting Zn/Cr ratio, a result similar to that previously reported by de Roy et al. [1]. However, decavanadate was incorporated even at pH 6.5 (if the decavanadate solution had been prepared at pH 4.5), but not at higher pH, probably due to the preferred formation of other oxovanadate oligomers. These authors also succeed to prepare by this direct method decavanadate intercalated Zn,Al LDHs, avoiding the use of ZnO.

Exchange of decavanadate by carbonate in the interlayer space of Mg–Al LDH was easily achieved by ultrasonic treatment of a suspension of the carbonate form in a vanadate solution at the pH required to polymerize VO_3^-, but without any further pH control [150]. It is likely that decavanadate exchange is facilitated by the high dispersion of the agglomerated particles following ultrasonic treatment, and also by enhanced diffusion of decavanadate on temporary delaminated particles.

Conductivity measurements have shown [151] that chloride/decavanadate exchange follows a first-order mechanism, without defoliation of the layered material.

In many of the synthesis leading to oxometalate–LDH compounds, in addition to the layered material containing decavanadate and characterized by a basal spacing close to 12 Å, an additional non-layered material, characterized by a broad diffraction peak close to 10 Å (in some cases, obscuring the first harmonic of the layered material), is formed [149,152–154], and is thought to be due to a compound formed as a result of the reaction between the basic hydrotalcite and the acidic polyoxometalate.

Anionic exchange of decavanadate for carbonate in LDHs containing Ni–Al or Mg–Al, with variable layer charge (M^{II}/M^{III} ratio ranging from 2 to 6) was attempted by Kooli et al. [155] by direct exposure of the LDH to a vanadate solution at pH 4.5. For the carbonate precursors, increasing amounts of Al led to a decrease in the a-parameter (lower ionic radii for Al^{3+} than for Mg^{2+} or Ni^{2+}) and a decrease in the c-parameter (lower electrostatic interaction between the increased positive layer charge and the carbonate anion [156]). Upon exchange, the crystallinity of the material decreases for M(Mg or Ni)/Al ratios larger than 4, and in the case of the Mg,Al LDH, the non-layered by-product, characterized by the diffraction peak close to 10 Å, also develops. It is expected that the V content depends on the M/Al ratio, and this is true for the Ni–Al series; however, it remains constant for the Mg–Al system, i.e. the exchange process results in a change in the Mg/Al ratio. From the value of the a-parameter, a value of 2 was calculated for the Mg/Al ratio, suggesting a dissolution of octahedral cations until a layer composition close to this value is obtained.

The synthesis of decavanadate-containing Mg–Al LDHs was studied by Ulibarri et al. [157,158] following different routes, Fig. 15: exchange of the initial carbonate or therephtalate anions, as well as reconstruction (directly to the vanadate form, or via intermediate terephthalate) of the layered structure from the carbonate form previously calcined at 550°C, also checking the role of preswelling with glycerol. In all cases a layered material containing $V_{10}O_{28}^{6-}$ was obtained (and, when used, therephtalate or glycerol were completely removed), together with the non-layered solid characterized by a XRD peak at 10 Å, but direct reconstruction of the calcined carbonate led also to formation of a fibrous material, and partial dissolution of Mg. The main difference in the properties of the solids obtained by the different routes corresponds to the pore size distribution, a narrow distribution being present in samples prepared via the terephthalate intermediate. The use of large organic anions as pre-swelling purposes to intercalate polyoxometalates has been claimed [50] as the most promising method for creating stable pores, avoiding the formation of sidephases. Similar methods were successfully used also by Chisem and Jones [159] to prepare decavanadate-containing Li–Al LDHs.

The Ni–Al LDH containing carbonate has been also pillared with polyvanadate at pH 4.5–5.5 by anionic exchange, without any swelling agent [160,161], and also by reconstruction of the carbonate form after calcination. However, exchange was only achieved when the Ni,Al LDH was maintained in solution (not dried) and the vanadate solution at pH 4.5–5.5 added, and not when a dried Ni–Al LDH was used. The same effect of the drying step was observed by Carrado et al. [95] for CuPcTs exchange in a Mg,Al–LDH. At pH 8.5 no exchange was observed, but at intermediate pH a biphasic material, with characteristic XRD peaks at 7.54 Å (carbonate) and 11.7 Å (decavanadate), was obtained. With regards to the reconstruction method, this was valid only if the sample was submitted to hydrothermal treatment at autogenous pressure, and when the precursor had been calcined at 300°C, but for higher calcination temperatures, NiO was also formed. According to Clause et al. [162], as the calcination temperature is increased, Al^{3+} ions migrate from the mixed oxide phase formed upon carbonate removal, to the crystallite surface, where from they are dissolved when the solid is suspended at pH 4.5; so, the nickel in excess does not enter the reconstructed LDH structure, but remains as an independent NiO phase. The intensities of the NiO XRD peaks decrease (and those of the LDH material increase) as the temperature during hydrothermal treatment is increased in the 80–150°C range. While at pH 4.5–5.5 reconstruction leads to the decavanadate–LDH phase (together with the byproduct responsible for the XRD peak at 10 Å), when the pH during reconstruction was increased the IR and XRD data indicate formation of (VO_3) chain-like polymeric metavanadate, composed of $[VO_4]$ tetrahedra with C_{2v} symmetry, and with the longitudinal chain axis parallel to the host layers.

Similar studies were also carried out with the Mg,Cr and Ni,Cr systems [161,163], but decavanadate-containing LDHs were obtained only when following the exchange method using pre-wet carbonate–LDH, and at pH lower than 6.5 for

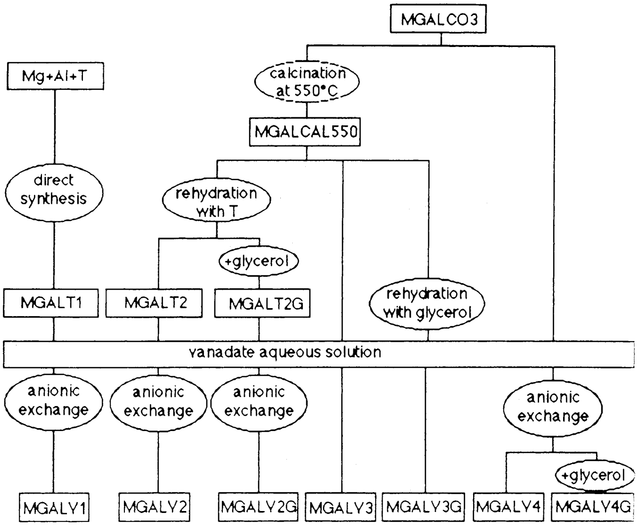

Fig. 15. Diagram showing various routes followed for the synthesis of terephthalate and vanadate materials. Reprinted from M.A. Ulibarri, F.M. Labajos, V. Rives, R. Trujillano, W. Kagunya, W. Jones, Comparative study of the synthesis and properties of vanadate-exchanged layered double hydroxides, Inorg. Chem. 33 (1994) 2592–2599, © 1994, with permission from The American Chemical Society.

Mg,Cr, but 5.5 for Ni,Cr. In other words, not only pH, but also the intrinsic nature of the layer cations seems to play an important role on the ability to exchange decavanadate for carbonate. With regards to vanadate-containing LDHs prepared following the reconstruction method, differences are also observed depending on the nature of the cations in the brucite-like layers. So, the Ni,Al and Mg,Cr systems are easily reconstructed if the carbonate precursor had been calcined below 300°C, while after calcination at 400°C only an amorphous material was obtained after contacting the calcined product with the vanadate solution. However, the Ni,Cr calcined precursor does not reconstruct at all, and the spinel ($NiCr_2O_4$) phase is detected by XRD in the precursor calcined at 500°C. Probably, the additional stability of the calcined product because of crystal field effects when containing transition metal cations somewhat hinders recovering of the layered structure with interlayer vanadates.

3.2.2. Thermal decomposition

Evolution of intercalated decavanadate to other species by thermal treatment has been widely studied, as interest in these polyoxometalate–hydrotalcite materials also stems from their potential use as catalytic materials, as prepared or after thermal decomposition [123,164]; already in 1984, they were reported to be useful for exhaust gas and hydrocarbon conversion processes [145]. Kagunya and Jones [165] have reported aldol condensation of acetaldehyde on a Mg,Al–vanadate LDH calcined at 450°C, although the activity is lower than in solids prepared, at the same temperature, from a carbonate precursor, probably because of a decrease in surface basicity, required for self-condensation of acetaldehyde.

Formation of cyclic and chain-like oxovanadates in the interlayers of a Mg,Al–LDH on heating at moderate temperatures has been reported by Twu and Dutta [139]. For the synthesis, these authors followed the two-step method [65], first preparing a Mg,Al–terephthalate LDH, then exchanging with $NaVO_3$ at pH 4.5. The nature of the intercalated anion was concluded not only from swelling, as measured by XRD, but also from Raman and XANES spectra. As the calcination temperature is increased, the gallery height, calculated from the position of the basal XRD lines, decreases; changes in the Raman spectra are consistent with the following series of reactions:

1. at 160–280°C: $V_{10}O_{28}^{6-} + 3H_2O \rightarrow 3V_3O_9^{3-} + HVO_4^{2-} + 5H^+$ although bands due to VO_4^{3-} (formed through deprotonation of HVO_4^{2-}) were also detected.
2. between 220 and 450°C: $nV_3O_9^{3-} \rightarrow 3n(VO_3)_n^{n-}$
3. between 450 and 650°C: $MgO + (VO_3)_n^{n-} \rightarrow \alpha\text{-}Mg_2V_2O_7 + Mg_3(VO_4)_2$

The XANES spectra [139] in the vanadium K-edge shows a pre-edge absorption (which intensity increases with the calcination temperature), assigned to a dipole forbidden 1s → 3d transition, strengthed by the mixing of the 3d orbitals with 4p metal and 2p oxide orbitals; this mixing is promoted by the lowering of symmetry around the vanadium atom from strictly octahedral (as that existing in decavanadate) to tetrahedral, existing in other vanadates.

The nature of the magnesium vanadate species formed upon calcination at high (700°C) temperature depends markedly on the nature of the precursor layered materials. So, calcination of a carbonate LDH containing Mg^{2+}, Al^{3+} and V^{3+} in the layers [166,167] leads mostly to formation of $Mg_3(VO_4)_2$ species, containing isolated $[VO_4]$ tetrahedra, while starting from a Mg,Al–LDH containing interlayer decavanadate [158,167] leads to formation of MgV_2O_6, containing pairs of edge-sharing VO_6 octahedra [168]. These results may be important for catalytic purposes, as it has been claimed [169,170] that the catalytic properties of the V–Mg–O system in the oxidative dehydrogenation of propane depend on the nature of the species existing, the highest selectivity being related to the presence of isolated $[VO_4]$ tetrahedra, the lack of V–O–V species (where oxygen can be released easily through reduction of V^{5+} to V^{4+}) decreasing the activity for combustion [171].

When the nature of the cations existing in the brucite-like layers is changed, the trends found are similar, although the calcination temperatures required for decomposition and crystallization of new phases may vary from one case to another: so, alumina-supported decavanadate maintains its structure up to 450°C [172,173]; when intercalated in Mg,Al LDH its decomposition starts at 100°C [139,174], but at 200°C in Ni,Al LDH prepared by ionic exchange, and at 150°C in the case of vanadate-containing Ni,Al–LDH prepared by reconstruction [160], and in Mg,Cr or Ni,Cr LDHs. Such a behavior can be related to hydrolysis of decavanadate species by water molecules remaining in the interlayer space, leading to polymers with lower charge density; the presence of cations with different polarizing power in the brucite-like layers would also modify the interaction between water molecules and the decavanadate anions. Surface acidity of the solids obtained upon calcination at 300 or 500°C of NiAl, NiCr, and MgCr LDHs containing decavanadate, has been assessed from IR monitoring of pyridine adsorption [175]. It has been found that samples NiAlV contain both Lewis and Brönsted acid sites, while Lewis sites are lacking in the presence of Cr. Adsorption of 2-propanol on these oxides takes place dissociatively, leading to oxidation to acetone at 300°C via a Mars and van Krevelen mechanism, more extensively in the less acidic, Cr-containing catalysts, although in this case further oxidation to acetate species takes place.

Twu and Dutta [135] have followed the evolution of $V_2O_7^{4-}$, exchanged at pH 10 in a Li,Al LDH, upon heating. In this case, heating at 80°C is enough to yield dimerization to $V_4O_{12}^{4-}$, but the process is reversible. Upon heating at 200°C hydroxide-mediated polymerization/depolymerization reactions occur, leading to oligomeric chains of $[VO_4]$ tetrahedra linked by oxygen atoms, which presence has been also ascertained by diffuse reflectance spectroscopy. Finally, above 450°C the Li aluminate framework is destroyed, forming Li_3VO_4 and $LiVO_3$. Oxidation of *o*-xylene on the material calcined at 450°C led to formation of *o*-tolualdehyde, indicating some sort of selectivity in oxidation of one of the methyl groups.

Thermal treatment may lead, in other cases, to different processes. So, on heating a $Ni^{II}Co^{III}$–LDH containing interlayer $(VO_3)_n^{n-}$ chains at 190°C (a temperature low enough to avoid collapsing of the layered structure), the basal spacing decreases from 9.15 to 7.21 Å, a value of the same order as that found with intercalated chromate and dichromate [127,128,131], and slightly smaller than that found for materials containing planar, interlayer carbonate; in other words, only a layer of oxygens, from the vanadate species, should be located between the hydroxide layers. This behavior has been ascribed to grafting of the intercalated anions to the layer upon heating, Fig. 11 [176]. The grafting process has been followed also by ^{51}V MAS-NMR, even from the very first stages of exchange in a $Ni^{II}Co^{III}$–LDH [177]; as soon as they are inserted in the interlayer to compensate the positive charge in excess in the layers, the isolated diperoxovanadate ions (formed in the NH_4VO_3/H_2O_2 medium) undergo a competition between polycondensation and grafting: if the solid is maintained with the reducing solution for a long time, partial grafting occurs, leading to dehydroxylation of the layers; however, if the solid is removed early from the solution, polycondensation is favored, together with a low extended grafting. Thermal treatment favors further grafting and defragmentation of the polyoxovanadate, finally leading to collapsing of the layered structure. Grafting (as concluded from an abnormal short layer–layer distance), even without any thermal treatment, has been also observed for pyrovanadate species, $V_2O_7^{4-}$, onto a Cu,Cr LDH [141]; in this case, however, two adjacent hydroxyl groups of one OH layer are substituted by two oxygen atoms of the ditetrahedra, as proposed also for a Cu,Cr–Cr_2O_7 LDH phase [128].

Isopolyvanadate has been also exchanged at pH 4.5 in Mg–Al LDHs in the nitrate form. A detailed study by XRD and IR spectroscopy of the species formed upon heating in air at increasing temperatures has been carried out by López-Salinas and Ono [174]. The results were similar to those reported by Twu and Dutta [139], despite the difference in the Mg/Al ratio, 2 or 3. The changes can be also easily followed by IR spectroscopy: The decavanadate gives rise to a strong, sharp absorption band at 957 cm^{-1}, together with weaker bands at 557, 598, 660, 740, and 820 cm^{-1}, while the presence of metavanadates gives rise to bands at 840 and 920 cm^{-1} (terminal V=O stretching), and 550 and 680 cm^{-1} (V–O stretching in bridging V–O–V bonds) [178]. If decomposition is carried out under vacuum, partial reduction of V^{5+} to V^{4+} species takes place, the highest concentration (6 $V^{4+}/100\ V_{total}$) of reduced species being reached at 150°C [174]; such a reduction is not reversed by oxygen treatment at 200°C during 1 h, probably because of the hindered access of even small molecules into the interlayer space due to very close adjacent isopolyanions.

The presence of decavanadate anions in the interlayer space of LDHs has also important effects on the decomposition process of the material. First of all, calcination of a Mg–Al LDH in the carbonate form usually leads to a weight loss close to 35–50% of the initial weight, due to removal of water physically adsorbed on the external surface of the crystallites (usually at low temperature), removal of interlayer water molecules, and, finally, dehydration/dehydroxylation, due to condensation of hydroxyl groups from the brucite-like layers, and decarbonation, from the interlayer carbonate anions [179,180]. If decavanadate, instead of carbonate, is present in the interlayer, the second weight loss corresponds only to water removal through condensation of layer hydroxyl groups, and the total weight loss is usually lower than 20–25% of the initial sample weight. The nature of the solids formed upon calcination also depends on the nature of the interlayer anion. This effect has been particularly studied for Co,Cr [181] and Zn,Cr [182] LDHs by del Arco et al. For Co,Cr–$V_{10}O_{28}^{6-}$ and Zn,Cr–$V_{10}O_{28}^{6-}$ LDHs prepared from a carbonate precur-

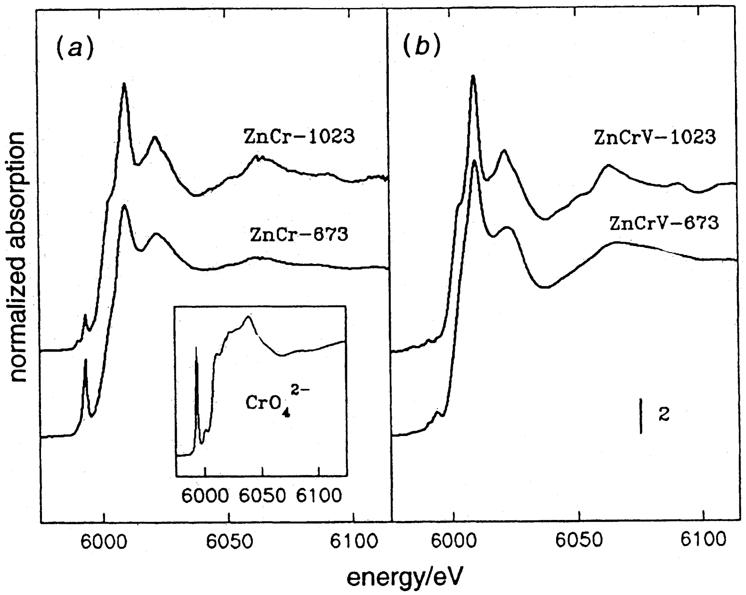

Fig. 16. Cr–K edges XANES spectra for Zn,Cr–CO_3 (a) and Zn,Cr–$V_{10}O_{28}$ (b) LDHs calcined at 400 and 800°C. Inset: Cr K-XANES spectrum for crystalline K_2CrO_4. Reprinted from M. del Arco, V. Rives, R. Trujillano, P. Malet, Thermal behaviour of Zn–Cr layered double hydroxides with hydrotalcite-like structures containing carbonate or decavanadate, J. Mater. Chem. 6 (1996) 1419–1428, © 1996, with permission from The Royal Society of Chemistry.

sor by ion exchange at pH 4.5, the XANES at the vanadium K-edge features (e.g. pre-edge peak intensity and position, main edge position, and post-edge structure) are almost identical as for a crystalline decavanadate (n-$C_6H_{13}NH_3)_6(V_{10}O_{28})\cdot 2H_2O$, confirming the structure of the intercalated anion. It has been also observed, from XAS studies [147], that the zinc shell is in accordance with Lowenstein's rule, which states that trivalent cations in aluminosilicates should not be in adjacent metal sites [183]. On calcination, while the DTA profiles for these carbonate LDHs showed the expected endothermic peaks due to water removal, when recorded in air, an additional exothermic peak was recorded for the Zn,Cr–LDH at 435°C (335°C for the Co,Cr–LDH), but was absent when recorded in nitrogen, indicating an oxidation process, involving the Cr ions; according to Fuda et al. [184], the presence of carbonate in the interlayer of hydrotalcites favors the $Cr^{3+} \rightarrow Cr^{6+}$ oxidation. The peak was absent in the DTA profiles of the vanadate-containing LDHs. When the samples were calcined in air at increasing temperatures, oxidation of Co^{2+} to Co^{3+} takes place at 400°C in the Co,Cr–CO_3 LDH, but not in the decavanadate analogue. In addition, a weak pre-edge peak characteristic of chromate ions appears at the chromium K-edge XANES spectrum, Fig. 16. Depolymerization of decavanadate species follows trends similar to those reported by Twu and Dutta [139] for Mg,Al–decavanadate LDHs. Calcination at 650°C leads to crystallization of $Co^{II}Co^{III}Cr^{III}O_4$ from the carbonate precursor, but of

$Co^{II}Cr_2O_4$ and $Co_2^{II}V_2O_7$ from the decavanadate precursor. In other words, the presence of decavanadate and the absence of carbonate hinders oxidation of Co^{2+} ions, thus modifying the nature of crystalline phases formed at high temperature. For the Zn,Cr analogues, the same behavior is observed with respect to Cr oxidation, and the crystalline phases formed were ZnO and $ZnCr_2O_4$ from the carbonate precursor (through formation of chromate species at intermediate calcination temperatures), and ZnV_2O_6 and $Zn_2V_2O_7$ at 400 and 750°C, respectively, from the vanadate precursor, together with $ZnCr_2O_4$. Formation of chromate and Co^{3+} species in the case of the carbonate precursors, but not in those containing interlayer decavanadate, has been also concluded from temperature-programmed reduction studies [181,182], a technique that has been proved to be adequate to determine redox processes in layered double hydroxides containing reducible cations in the layers or in the interlayer anions [185].

3.2.3. Molybdates

While the chemistry of vanadates in the interlayer space of LDHs has been throughout studied, that of molybdates has been restricted to the heptamolybdate, $Mo_7O_{24}^{6-}$, and the papers published are rather scarce. The preswelling technique with terephthalate was used by Drezdzon [65] to intercalate $Mo_7O_{24}^{6-}$ in the interlayer space of a Mg,Al carbonate precursor. The method was similar to that above described for decavanadate, i.e. direct preparation of the Mg,Al–terephthalate precursor (from Mg^{2+} and Al^{3+} nitrates and terephthalic acid in NaOH medium), and mixing of the slurry with a $Na_2MoO_4 \cdot 2H_2O$ aqueous solution, and further lowering of the pH to 4.4–4.7 with HNO_3. The basal spacing was 12.2 Å, corresponding to a heptamolybdate orientation in which the C_2 axis is perpendicular to the brucite-like layers. Exchange reactions using other organic precursors did not succeed (2,5-dihydroxy-1,4-benzendisulphonate; lauryl sulphate) or proceed with difficulty (1,5-naphtalenedisulphonate), because of competition with complex formation between the organic species and the metalate [186].

The so-called reconstruction method, from a carbonate precursor calcined at 450°C and an acidified (pH 4.5) solution of ammonium heptamolybdate, led also to intercalation of heptamolybdate species [148,187] with the same spacing as that obtained by Drezdzon. However, Misra and Perrotta have reported [126] the preparation of a Mg,Al–Mo_7O_{24} LDH with a basal spacing of 9.6 Å from a carbonate precursor calcined at 500°C, but without acidification. This spacing is markedly lower than that reported by Drezdzon for samples prepared by the terphthalate intermediate [65], and by Chibwe and Jones [148] for samples prepared by reconstruction. The difference has been attributed by these authors [126] to the different Mg/Al ratio in their sample (1.88) and in Drezdzon's sample (2.0). However, the difference is very small and, moreover, the value by Misra and Perrotta is almost coincident with that reported by Chibwe and Jones (1.82), which led an interlayer space of 12.0 Å. So, the difference should be more probably due to: (i) a different orientation of the interlayer anion, (ii) the presence of a different oxomolybdate anion (due to partial depolymerization), or (iii) some sort of grafting, as reported in the case of vanadate [141] and chromate [127,128,131], as remaining of organic molecules in the interlayer space should be ruled out since these were not used in the method followed by Chibwe and Jones [148]; unfortunately, these authors [126] provide no other experimental data, in addition to XRD, to support their conclusions. The same value, 12.0 Å, has been recently reported by Hibino and Tsunashima [188] for samples prepared in an ethanol–water solution by anionic exchange, to avoid partial dissolution of the brucite-like layers, due to the acidic medium provided by the molybdate solution. A value of 12.2 Å has been also reported [189] by Twu and Dutta in materials (Mg/Al = 2.0) prepared following the Drezdzon's method; although the layer structure is destroyed at 300°C, the $Mo_7O_{24}^{6-}$ moiety is stable up to 400°C, then forming $MgAl_2O_4$, $MgMo_2O_7$ and $MgMoO_4$, as concluded from XRD and Raman spectroscopy studies. However, intercalation of MoO_4^{2-} in a Li,Al LDH failed, due to hydrolysis of the molybdate anion, even at r.t.

Levin et al. [190,191] have reported synthesis of a layered ammonium zinc molybdate using as a precursor a Zn,Al–LDH calcined at 500°C and $Mo_7O_{24}^{6-}$ (although this depolymerizes along the reaction) at r.t. These authors find a similar reactivity with LDHs containing, in addition to Zn and Al, Cu^{2+}, Co^{2+} or Ni^{2+}, but not with LDHs containing Ni^{2+} or Mg^{2+} only as the divalent cation. From ^{27}Al MAS-NMR studies, it was concluded that a high fraction of tetrahedral Al^{3+} ions are required in the calcined precursor to yield the layered molybdate.

3.3. Layered double hydroxides intercalated with high-nuclearity oxometalates: iso and hetero-polyoxometalates

In this chapter we summarize the studies reported on the synthesis, characterization, and properties of LDHs where the anions existing in the interlayer space is a polyoxometalate (POM) possessing the Keggin-type, or related, larger structures, such as Dawson and Finke [192] or Preyssler types [193]. One of the aims of these studies was to expand the layers further than the values obtained with decavanadate; it has been also observed improved catalytic properties of these systems. In a Keggin-type structure, twelve metaloxygen octahedra form a shell surrounding a tetrahedrally coordinated heteroatom (P, Si, B, etc.); the shape is close to spherical, with a diameter of ca. 10 Å

Kwon and Pinnavaia [194] reported in 1989 the preparation of LDHs containing intercalated $[XM_{12}O_{40}]^{n-}$ anions. These pillared intercalates are intrinsically difficult to synthetize in highly crystalline form, in part, because LDH hosts are basic, whereas the anions are highly acidic. Actually, these authors succeed in preparing intercalates with a $Zn_2Al–NO_3$ precursor by ion exchange, but not with the more basic $Mg_3Al–NO_3$ one. The gallery height, as determined by XRD, was close to 10 Å, and the intercalation by ion exchange seems to depend on the net charge and on the polyhedral form of the anion. So, intercalation with a hot suspension of $Zn,Al–NO_3$ LDH (Zn:Al = 2:1) with α-$[H_2W_{12}O_{40}]^{6-}$ and α-$[SiV_3W_9O_{40}]^{7-}$ led to complete exchange, while exchange was lower than 20% for Keggin-type structures, such as $[PCuW_{11}O_{39}(H_2O)]^{5-}$, and no exchange at all was observed with α-$[PW_{12}O_{40}]^{3-}$ or α-$[SiW_{12}O_{40}]^{4-}$. These findings are in agreement with charge balance reasons: as the diameter of the Keggin unit is close to 9.8 Å, an area of 83 Å^2 is required to accomodate a Keggin unit; as the charge density in the LDH used was 16.6 Å^2 (although this value has been corrected to 25 Å^2 by Clearfield et al. [122]), those Keggin units with a formal charge lower than -5 will be unable to enter in the interlayer space to compensate the positive charge of the layers.

In any case, the products obtained, Zn,Al–α-$[H_2W_{12}O_{40}]^{6-}$ and Zn,Al–α-$[SiV_3W_9O_{40}]^{7-}$, are crystallographically well-ordered phases, with a basal spacing of 14.5 Å, corresponding to a gallery height of 9.8 Å, in agreement with crystallographic data for Keggin units, and up to six diffraction harmonics were recorded in the XRD diagram. The extremely large swelling of the layers is accompanied by a substantial increase in the specific surface area, from 26 m^2 g^{-1} for the nitrate precursor, to 63 and 155 m^2 g^{-1}, respectively, for the solids intercalated with α-$[H_2W_{12}O_{40}]^{6-}$ and α-$[SiV_3W_9O_{40}]^{7-}$, and then the term ‘pillared’ seems to be more adequately used than in other cases where, despite intercalation of large anions, such an increase is not observed. Further evidence for the retention of the Keggin structure inside the layers was attained by IR and ^{29}Si and ^{51}V MAS-NMR spectroscopies. With respect to the orientation of the anion in the interlayer, these authors [194] conclude that the C_2 axis of the oxygen framework should be perpendicular to the brucite-like layers, Fig. 17, as in this orientation the number of hydrogen bonds to layer OH groups is maximized. This orientation has been also proposed by Liu et al. [195] for $[PW_{11}O_{39}Cr(H_2O)]^{4-}$, $[PW_{11}TiO_{40}]^{5-}$ and $[PW_{11}VO_{40}]^{4-}$ intercalated in Zn,Al–LDHs prepared by ion exchange.

In order to intercalate Keggin-type anions in rather basic LDHs, Dimotakis and Pinnavaia have proposed [196,197] an alternative method, consisting in preparation of the Mg$_3$Al–OH LDH (meixnerite) by reconstruction of a calcined carbonate precursor; meixnerite is then exchanged with *p*-toluensulfonate or adipate in the presence of glycerol as a swelling agent, yielding a well-crystallized phase with extremely well ordered organic anions, which gallery height is very close (14.4 Å for the adipate) to that of the Keggin derivative, from which anion exchange led to microporous, single crystalline phases with $d = 14.8$ Å, after exchanging with $[H_2W_{12}O_{40}]^{6-}$ or $[SiW_{11}O_{39}]^{8-}$.

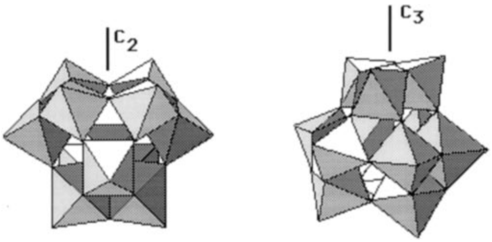

Fig. 17. A Keggin unit, $[XM_{12}O_{40}]^{n-}$, formed by 12-corner-sharing octahedra, in two different orientations.

The reconstruction method originally used by Chibwe and Jones to prepare LDHs by reconstruction of calcined precursors [148] has been tested by Narita et al. [152] to prepare intercalates with Keggin anions, starting from a Zn,Al–CO_3 precursor. Addition of the amorphous solid obtained after calcination at 500°C to a boiling solution of $[SiW_{11}O_{39}]^{8-}$ at pH 6 led to a LDH with a basal spacing of 14.6 Å, almost coincident with the value reported for the solid obtained by ionic exchange [194]. However, in addition, a broad reflection is also recorded at ca. 10.2 Å, which has been ascribed by these authors [152] to a quasicrystalline phase consisting of Zn^{2+} and Al^{3+} salts, and similar results were obtained for $[SiV_3W_9O_{40}]^{7-}$. Nevertheless, the method [148] seems to be general both for acidic and basic LDHs, although with acidic LDHs better ordered systems are obtained.

These authors have also prepared Zn,Al–LDHs intercalated with the Keggin ion α-$[SiW_{11}O_{39}]^{8-}$ by direct synthesis [153], i.e. by adding a solution of Zn^{2+} and Al^{3+} to a vigorously stirred solution (100°C, pH 6) of the Keggin species. Although the XRD diagram shows several sharp harmonics corresponding to (00l) diffractions (the first one at 14.6 Å, a value similar to that obtained for solids prepared by ion exchange or reconstruction [152,194,197]), the broad feature at ca. 10.8 Å is also observed for the solid prepared by reconstruction [152] by these same authors.

The use of swelling organic molecules (glycerol or triethylenglycol) to prepare the Mg,Al–$H_2W_{12}O_{40}^{6-}$ LDH has been also followed by Pinnavaia et al. [198]. The advantage of the method is the direct use of the carbonate form of the LDH precursor. Hansen and Taylor [199] had reported that the reaction of Mg,Al–CO_3 LDHs with glycerol at 160°C resulted in swelling and well dispersed LDH suspensions. Well crystallized LDHs have been obtained by Pinnavaia et al. following this method [198], with up to seven basal harmonics in their XRD diagram, and with a basal spacing of 14.9 Å, characteristic of LDHs intercalated with Keggin ions, Fig. 18. Although a byproduct, characterized by a broad diffraction at ca. 11 Å, is also formed, its content is lower when using triethyleneglycol than when using glycerol or in samples prepared by reconstruction [153]. Also, the particles show an irregular glass-like morphology, very different from the hexagonal morphology of the starting carbonate LDH, thus indicating the reaction is not topotactic (as observed in samples prepared by ionic exchange of a LDH–OH precursor), but probably proceeds via dissolution and recrystallization of the LDH–CO_3 at high temperature. Differences are observed also in the specific surface area and porosity of the samples: those prepared following the polyol route display a value of ca. 160 m^2 g^{-1} (83 m^2 g^{-1} when prepared by ion exchange of meixnerite), 65% of which corresponding to micropores. However, Weir et al. [200] have reported a total blocking of the micropore system of Mg,Ga and Mg,Al–LDH containing $[PW_{11}O_{39}]^{7-}$ and $[H_2W_{12}O_{40}]^{6-}$, prepared via terephthalate intermediates, probably because of the large charge density of the LDH–terephthalate precursors (Mg^{2+}:M^{3+} = 2:1).

Clearfield et al. have carried out a detailed study on the experimental conditions to intercalate Keggin anions in LDHs [122,154]. These authors have prepared different LDHs precursors, Mg_mAl–X ($m = 2$–5; X = Cl^-, NO_3^-) pillared with $[PV_nW_{12-n}O_{40}]^{(3+n)-}$ ($n = 0$–4), and have shown that exchange can be attained in

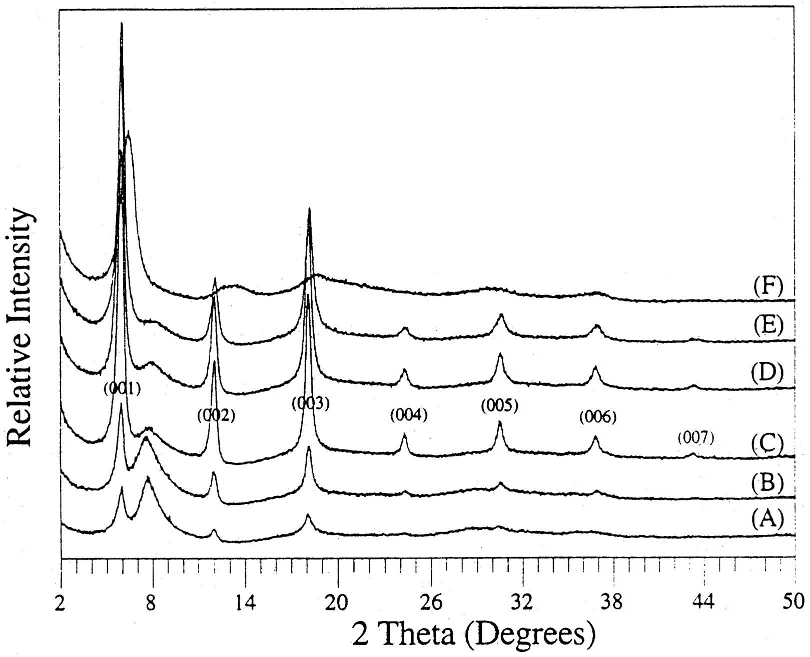

Fig. 18. XRD patterns (Cu–K_α) of oriented film samples of Mg,Al–LDH metatungstate reaction products obtained from (A) meixnerite, (B) LDH glycerolate, and (C) LDH triethyleneglycolate precursors. All diffraction patterns were recorded at r.t. For the LDH–POM intercalated derived from the triethyleneglycolate precursors, the XRDs were taken at r.t. after 1 h preheating under nitrogen at (D) 100, (E) 200, and (F) 250°C. Reprinted from S.K. Yun, V.R.L. Constantino, T.J. Pinnavaia, New polyol route to keggin ion-pillared layered double hydroxides, Microporous Mater. 4 (1995) 21–29, © 1995, with permission from Elsevier Science.

aqueous solution without any organic swelling agent. Direct anion exchange in aqueous solution was also used by Guo et al. [201] to prepare Zn_2Al–LDH intercalated with $[PV_nW_{12-n}O_{40}]^{(3+n)-}$ ($n = 1$–4). Exchange is easier if the LDH precursor is thoroughly wet [122,154], either by preparing wet solids or by soaking the dried product for 3–4 h (a similar role of the wetness state of the precursor has been also shown by Carrado et al. [95] and Kooli and Jones [149] to incorporate phtalocyanines or decavanadate in the interlayer region, respectively). Also the exchange is easier with soft powders than with glassy particles. Moreover, if the solid is slurried enough, pillaring seems to be almost independent on the charge of the Keggin unit: for a wet Ni_2Al–NO_3 precursor soaked for at least 3 h, total exchange was obtained with all Keggin ions with net charge ranging from -3 to -7 (a 90% exchange was already attained after 5–10 min). This apparent independence on the net charge of the Keggin unit is rather surprising, as the area required to accomodate a Keggin unit is 83 Å^2, and the area per layer charge unit is 25 Å^2 (16.6 Å^2 according to Kwon and Pinnavaia [194]); then the charge per Keggin unit should be, at least, -4 (or -5, according to Kwon and Pinnavaia). The experimental finding that even Keggin units with a net charge of −3 are also exchanged, can be only explained assuming an alteration of the layers during the exchange process, leading to an increase in the layer charge density.

On the other hand, the interlayer spacing required to host the Keggin unit is close to 14.2 Å, but the interlayer spacing measured for the pillared Ni,Al–LDHs was only ca. 12 Å. For the Mg,Al–LDHs the spacing was 14.7 Å (the corresponding harmonics being also recorded), and an additional broad reflection, similar to that reported by Narita et al. [152], was also recorded at 11–13 Å. These authors suggest a partial dissolution of the divalent anion in the acidic medium (pH 4–5) during exchange, together with partial removal of hydroxyl groups from the layers, thus creating vacancies where the Keggin ions could fit, leading to interlayer spacings lower than expected, and thus explaining intercalation of the $[PW_{12}O_{40}]^{3-}$ Keggin unit. Computer graphics models support such relationship between ‘penetration’ of the Keggin units into the brucite-like layers, and the spacing.

To overcome the difficulty in intercalation of Keggin units with low negative charge, Serwicka et al. [202] have subjected the $[PMo_{12}O_{40}]^{3-}$ anion to electrochemical reduction prior to exposure to the LDH; it is known [192] that these anions undergo facile reduction to give so-called heteropoly-blues, and that reduction renders the anions less acidic, so helping also to overcome decomposition by the reaction with the rather basic Mg,Al–NO_3 LDH. In this case, reduction led to a transfer of four electrons to the Keggin unit, and the authors find that the unreduced heteropolyanion actually reacts with the LDH, XRD show diffraction maxima at 11.1 Å, too small to correspond to the intercalated Keggin unit, probably corresponding to decomposed species; the atomic Mo:P ratio was 4.5. However, for the reduced heteropolyanion, the spacing was 14.8 Å, with corresponding harmonics, although an intense reflection was also recorded at 10.8 Å, ascribed to formation of a non-layered byproduct.

Direct exchange reaction in aqueous solution has been used by Hua et al. [203,204] to intercalate peroxoheteropolyanions with the Keggin structure, such as $[SiW_{11}(TiO_2)O_{39}]^{6-}$, $[SiW_9(TiO_2)_3O_{37}]^{10-}$, $[PW_{11}(TiO_2)O_{39}]^{5-}$ and $[PW_9(TiO_2)_3O_{37}]^{9-}$, in Zn_2Al–LDHs in the nitrate form, obtaining solids with basal spacings of 14.7 Å.

Weber et al. [205] have studied by TEM the partial exchange of $[SiV_3W_9O_{40}]^{7-}$ in a Mg_2Al–LDH. These authors find that the average crystallite size of the exchanged product was larger than that of the original LDH, suggesting exchange proceeds via dissolution and topotactic reprecipitation of the exchanged LDH, as also proposed by Pinnavaia et al. when following formation of triethylenglycol intermediates [198]. On the other hand, the results obtained on the local chemical composition (Mg/Al and W/Al ratios) indicate that in partially intercalated solids, the resulting structures consist of stacks of completely substituted layers superposed on unchanged layers.

The synthesis of many other LDHs containing intercalated Keggin-type anions has been described in the literature. Hu et al. [206,207] have reported the intercalation in Zn_2Al–LDH of different POMs, such as $[PVW_{11}O_{40}]^{4-}$, $[XW_{11}O_{39}Z(H_2O)]^{n-}$ ($X = Si$, B; $Z = Co$, Ni, Cu, Al), $[Ln(XW_{11}O_{39})_2]^{n-}$ ($Ln = La$,

Ce^{III}; X = Si, P, B) by ion exchange. As expected, basal spacings close to 14.5 Å were observed and, from ^{31}P and ^{27}Al MAS-NMR, orientation of the Keggin unit with its C_2 axis perpendicular to the layers was concluded, validating the prediction made by Pinnavaia et al. based on the formation of hydrogen bonds between the layers and the oxide ions of the Keggin unit [194]. $[SiW_{11}O_{39}Co(H_2O)]^{6-}$ was intercalated in the interlayer space of Zn_2Al-NO_3 LDH by the action of ultrasound [208], a method previously used to intercalate decavanadate [151].

López-Salinas et al. have reported [209] the intercalation of $[SiW_{11}O_{39}X(H_2O)]^{6-}$ ($X = Co^{2+}$, Mn^{2+}) in a Mg_2Al-NO_3 LDH by ion exchange, obtaining a layered material with a basal spacing of 15.2 Å, although a byproduct, characterized by the broad reflection close to 11 Å, is also formed. The structure is stable up to 350°C, and the water ligand can be reversibly removed below 200°C. The coordinatively unsaturated cation (Co or Mn) can reversibly adsorb small molecules, such as water, methanol, ethanol or ammonia, as concluded from UV–vis/DR studies, while no spectral changes were observed upon adsorption of pyridine (vapor or liquid phase) or THF, probably because of steric hinderance to access the adsorption site.

Clearfield et al. [38] have described the synthesis of a Cu,Al–LDH intercalated with the $[PV_3W_9O_{40}]^{6-}$ anion by a controlled increase of the pH of a solution containing the POM and the metal cations (Cu^{2+} and Al^{3+}), via hydrolysis of urea on mild heating (ca. 50°C). The method permits a completely homogeneous pH environment throughout the solution, avoiding local changes in concentration, pH, etc.

Intercalation of heteropolyanions larger than Keggin-type ones has been reported by Yun and Pinnavaia [210]. These authors report intercalation of anions with Dawson, α-$[P_2W_{18}O_{62}]^{6-}$, and Finke, $[Co_4(H_2O)_2(PW_9O_{34})_2]^{10-}$, structures in a Mg_3Al–LDH, and compare the results with intercalation of the Keggin ion α-$[H_2W_{12}O_{40}]^{6-}$. In addition to obtaining larger gallery heights, differences are also found due to different orientations that these anions can achieve in the interlayer space, as, contrary to the spherical shape shown by the Keggin ions, the Dawson and Finke ions have a structure close to cylindrical (D_{3h} and C_{2h} symmetry, respectively), so the size of micropores could be hopefully modulated. The Dawson and Finke derivatives were prepared using a LDH–adipate as the precursor at 100°C, following the method by Dimotakis and Pinnavaia [196], and also using a meixnerite precursor and ambient pH conditions at r.t. [210]. With respect to the Dawson derivatives, the first method yielded a layered material with a basal spacing of 17.6 Å, suggesting the anion is oriented with its C_2 axis perpendicular to the layers; only small decreases in the basal spacings are observed when the solid is heated at 25–200°C, probably due to dehydration. However, via the meixnerite method, the basal spacing was 19.3 Å, in agreement with the C_3 axis of the anion perpendicular to the layers; this value decreases irreversibly to 17.4 Å upon heating at 100°C, suggesting a re-orientation of the Dawson unit from end-on position to an horizontal position, Fig. 19; the former orientation seems so to be unstable, and, actually, while only six oxygen atoms from the Dawson unit are oriented to form hydrogen bonds with the layers in the end-on position, in the horizontal position 14 oxygen ions are able.

Contrary to the results with the Dawson's anion, intercalation of the Finke anion led to layered materials with a basal spacing of 17.7 ± 0.3 Å, whichever (adipate or meixnerite) the precursor used, suggesting that both intercalated products have the C_2 axis of the heteropolyanion perpendicular to the LDH layers. The microporous structure is maintaned up to 200°C when heated in N_2. Upon heating, the gallery height decreases by 2–3 Å, by removal of water molecules, resulting in stronger electrostatic and hydrogen bonding interactions between the oxygen ions of the heteropolyanion and the LDH hydroxyl groups, leading to reorientation of the former. Retention of the Dawson and Finke structures in the intercalated state was verified by FTIR spectra, which showed the expected bands due to P–O linkages close to 1100 and 1030 cm^{-1}, and W–O linkages close to 960, 930, and 750 cm^{-1}, the precise positions depending on the particular POM [211,212].

As in most of the cases previously described [153,154,205], the XRD diagrams of these materials showed, in addition to the lines due to the layered material, a broad peak close to 11 Å. Although different explanations have been previously proposed for the nature and origin of the material responsible for this reflection, these authors conclude that salt formation from cations depleted from the layers and non-gallery POM remains the favored explanation, and the XRD features of this impurity were the same as of the solid obtained by grinding a carbonate–LDH or even $Mg(OH)_2$ and a POM in the solid state. This report [210] represents the most widely study on this byproduct, detected upon reaction of POMs with LDHs.

Larger POMs have been introduced in the gallery space of Mg,Al and Zn,Al LDHs by Evans et al. [147] by ion exchange and direct synthesis; solids have been prepared with gallery heights ranging from 7.1 to 16 Å including species such as $[Nb_xW_{6-x}O_{19}]^{(x+2)-}$ ($x = 2$–4), $[V_2W_4O_{19}]^{4-}$, $[Ti_2W_{10}PO_{40}]^{7-}$, and $[NaP_5W_{30}O_{110}]^{14-}$. The largest yields to highly crystalline solids were obtained following the exchange method, with precursors containing chloride or nitrate.

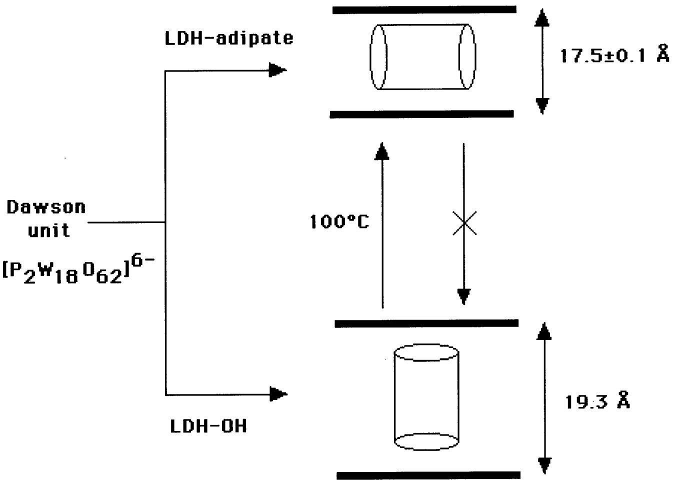

Fig. 19. Reaction scheme for intercalation of Dawson polyoxometalate in a LDH.

These POMs, in addition, are stable in a wide pH range, and so can be incorporated into the interlayer space of strongly basic Mg,Al–LDH. Probably, one of the most interesting products prepared by these authors [147] is that containing the Preyssler anion, $[NaP_5W_{30}O_{110}]^{14-}$, one of the largest known anions, and a rather abnormal chemical assembly with a C_5 axis. Its structure consists of a cyclic arrangement of five $[PW_6O_{22}]$ units, each formally derived from the Keggin-type ion $[PW_{12}O_{40}]^{3-}$ by removal of two sets of corner-shared $[WO_6]$ groups. The basal spacing for the Zn,Al–Preyssler derivative obtained from the nitrate precursor was 21 Å, in agreement with the ion orienting its shortest dimension parallel to the host layers. When ion exchange was performed from benzenecarboxylate-containing precursors ($YC_6H_4COO^-$, $Y = COO^-$, OH, CH_3), low (ca. 3.5–4.5) pH values were required to protonate the carboxylate group, to induce removal of the free organic acid. Direct synthesis led to incorporation of the Preyssler ion in a Zn,Al–LDH, with a spacing of 21 Å. Retaining of the POM structure was checked by EXAFS [147]. As expected, a by-product responsible for a reflection at 7–11° (2θ, Cu–K_α) and which nature has been discussed above is formed in most of the cases.

Studies on the thermal decomposition of Zn_2Al–LDHs intercalated with different Keggin ions have shown [213] that after dehydration (200°C), dehydroxylation is completed at 350°C, leading to amorphous solids; the layer structure is destroyed between 200 and 250°C, depending on the precise nature of the interlayer Keggin ion. The layered material can be rehydrated by immersion of the calcined solid in water, but the pillared, layered structure is not reconstructed by simply rehydration. Crystallization of anhydrous mixed oxides (e.g. $ZnWO_4$) is observed after dehydroxylation, leading to an exothermic peak in the DSC trace. Similar results have been reported by Guo et al. [214].

The structure of salts of Keggin ions with bulk cations (e.g. $Cs_3[PW_{12}O_{40}]$) is stable even up to 700°C. The results by Kwon and Pinnavaia [213] suggest that the mixed oxide formed upon decomposition of the brucite-like layers reacts easily with the hosted Keggin ion. This low thermal stability in some sort of way limits the application of these materials to catalytic processes taking place at rather low or even r.t., such as photocatalytic oxidation of isopropanol to acetone [213].

Although LDHs are mostly basic solids, incorporation of POMs in the interlayer space not only increases the gallergy height and the thermal stability, but also may provide electron acceptor sites and acid sites. Thereof, these LDH–POM compounds are interesting because of their acid–base properties. In these LDH–POM systems, basic sites are located on the layers, while acid sites are on the interlayer anions [215]. As a consequence, the relative acid–base strength could be changed by different anionic exchange ratios, or even thermal treatments to yield materials with tailored acid–base properties. Putyera et al. [216] have prepared a series of Mg,Al–LDHs intercalated with molybdate and tungstate, in order to assess the relationship existing between the composition and the acid–base properties of the pillared materials and of their derivatives obtained upon calcination. As expected, bearing in mind the close relationship existing between the nuclearity of the POM and the pH, (WO_4^{2-} is stable at $pH > 8$, $W_{12}O_{42}^{12-}$ at pH 7.8, and $W_{12}O_{39}^{6-}$ at pH

5.7, while for the oxomolybdate species, MoO_4^{2-} is stable at pH > 7, but $Mo_7O_{24}^{6-}$ at lower pH values), a change in pH during synthesis gives rise to different acid sites/basic sites ratio in the intercalated derivatives. Upon calcination, formation of high nuclearity oxometalates ($Mo_7O_{24}^{6-}$ or $W_{12}O_{41}^{10-}$) again produces changes in the acid–base properties.

Polyoxometalates are well known as oxidation catalysts, and so it is expected that POM-catalyzed oxidation processes on POM hosted in the interlayer region of an LDH can be constrained in a shape-selective environment. Tatsumi et al. [217,218] have reported the epoxidation of alkenes (e.g. 2-hexene, cyclohexene and β-methylstyrene) with H_2O_2, catalyzed by LDHs intercalated with POM derivatives of Mo and W. When the catalytic activity results are compared with those for the unhosted POM, an steric effect is observed, and so epoxidation of large alkenes is less favored on the LDH–POM catalyst, than when smaller alkenes are used. On the other hand, the steric hinderance for the alkenes to access the interlayer region seems to be less important for LDH–$W_{12}O_{41}$ than for LDH–Mo_7O_{24}, in agreement with a larger basal spacing in the former than in the latter (12.2 vs. 9.9 Å, respectively). These results suggest a possible shape selectivity control on changing the size of the hosted species. In addition, hydrolysis of epoxides to yield di-ol species is slowed down if compared with that observed for the unhosted catalysts, probably because of the basic properties of the brucite-like layers. However, Gardner and Pinnavaia have recently pointed out [219] that the co-product generally formed (characterized by a broad diffraction maximum close to 10–11 Å) when preparing LDH–POM intercalates can have important catalytic consequences, and be even catalytically more important than the LDH phase.

The catalytic oxidation of benzaldehyde to benzoic acid using H_2O_2 in a biphasic liquid–solid system, has been studied by Hu et al. [220] on Zn,Al–LDHs intercalated with $[SiW_{11}O_{39}]^{8-}$ and $[SiW_{11}O_{39}Z(H_2O)]^{6-}$ ($Z = Co^{2+}$, Ni^{2+}, Cu^{2+}). The largest catalytic activity has been observed for the cobalt-derivative, and this finding has been tentatively related to the easy change in the oxidation state of Co, suggesting that Co^{2+} becomes oxidized to Co^{3+} by H_2O_2, and Co^{3+} oxidizes benzaldehyde to benzoic acid.

Guo et al. [221] have studied the O_2-oxidation of cyclohexene on LDHs intercalated with $[XW_{11}O_{39}Z(H_2O)]^{n-}$ ($X = P$, Si; $Z = Mn^{2+}$, Fe^{3+}, Co^{2+}, Ni^{2+}, Cu^{2+}). The LDH–POM system is more active than the LDH in its nitrate form, and also more active than the alkaline salts of the POM. An effect of the transition metal cation existing in the POM moiety (Z) has been observed. It was concluded that the cations in the layers or in the POM group behave as active sites for oxygen transfer in cyclohexene oxidation, and so the catalytic properties could be hopefully tuned by precise changes in the nature and concentration of transition metal cations in both types of sites (layers and POM units).

Zheng et al. [222] have reported alkylation of iso-butane with butene on Zn,Al–LDHs intercalated with $[SiW_{12}O_{42}]^{8-}$, and of Ni,Al–LDH intercalated with $[PW_{12}O_{42}]^{7-}$, with good results with respect to activity and selectivity. For this reaction, alkylation may proceed on basic (LDH) or acid (POM) sites, i.e. the POM-pillared LDH can behave as a bifunctional acid–base catalyst. On calcination at 300°C, $Ni_2Al–PW_{12}O_{42}$ shows a much higher butene conversion than the uncalcined material, as well as a higher content of C_{12} and C_{16} products, probably due to a lower steric hinderance upon removal of interlayer water molecules.

Clearfield et al. [38] have used LDH–POM materials for catalytic conversion of isopropanol to acetone or propene. This is a test reaction widely used for catalyst characterization, as it proceeds to propene on acid sites, while to acetone on basic sites. According to these authors, LDHs such as $Mg,Al–CO_3$ behave as basic catalysts, leading to acetone [215]. However, insertion of heteropolyacid anions alters the selectivity drastically towards propene, showing that the acid character of the POM predominates. Minor changes in acid/base catalytic properties have been also correlated to the precise nature of the cations (Co^{2+}, Fe^{3+}, Ni^{2+}, Mg^{2+}, Al^{3+},...) in the brucite-like layers. Studies by Kagunya and Jones [165] on the aldol condensation of acetaldehyde on $Mg,Al[SiW_{12}O_{40}]$ have correlated the catalytic activity with the surface area available, while selectivity seems to be related to the number and strength of the basic sites, responsible for the activity in this reaction.

Ethanolysis of propene oxide to yield glycol ether (a reaction that can proceed catalytically both on acid and basic sites) has been studied by Jones et al. [223] as a way to assess the nature of active sites in Mg,Al–LDHs intercalated with POMs such as $[PW_{12}O_{40}]^{3-}$ and $[SiW_{12}O_{40}]^{4-}$. While for the LDHs lacking interlayer POMs these authors report the hydroxyl groups as being the active sites, in the LDH–POM systems, up to three sites are present: (i) oxide anions directly linked to metal atoms (strong basicity), (ii) oxide ions bonded to atoms adjacent to metal centers (medium basicity), and (iii) surface hydroxyl groups (weak basicity).

The acid–base functionality of the $Mg,Al–LDH–[H_2W_{12}O_{40}^{6-}]$ association, which synthesis has been described above, has been examined by Pinnavaia et al. [198] using 2-methyl-3-butyn-2-ol (MBOH) as a reactive probe. When the catalyst was obtained via a triethylenglycolate intermediate, a high reactivity for the base-catalyzed disproportionation was observed, whereas when obtained via the glycolate or meixnerite it was rather inactive. The difference has been attributed to the different porosity in the samples obtained when using alternative intermediates.

Keita et al. [224,225] have prepared oxometalate-clay-modified electrodes containing metatungstate. Glassy carbon electrodes have been modified with LDHs containing Zn and Al in the brucite-like layers, and the interlayer anions have been substituted for $[H_2W_{12}O_{40}]^{6-}$ under mild acid conditions. Clay films were prepared by dropping a colloidal solution of the LDH onto the glassy carbon surface; incorporation of the POM was accomplished readily by cycling the electrode in the solution containing the oxometalate in the potential domain of the first redox system of $[H_2W_{12}O_{40}]^{6-}$ to monitor the progress of the incorporation. Migration of the highly-charged POM in the interlayer region of the clay results in the final LDH–POM system. The best results were obtained with a Zn,Al–LDH precursor containing the relatively large (if compared to chloride or nitrate) terephthalate dianion at pH 5, acidic enough to ensure protonation of the organic anion (thus favoring its removal from the interlayer region), but basic enough to avoid dissolution of the layers.

4. Miscellaneous

Adsorption of several oxometalates on mixed oxides prepared by calcination of hydrotalcites (originally containing carbonate in the interlayer space) has been studied as a way to remove these anions from waste water. Sato et al. [226] have reported the adsorption of CrO_4^{2-}, HVO_4^{2-}, and MnO_4^-, among other oxoanions, on a Mg,Al–LDH previously calcined at 500°C. The degree of adsorption of divalent anions was greater than that of monovalent anions, although longer equilibrium times were required to reach the equilibrium. Similar results have been more recently reported by Rhee et al. [227] for chromate sorption on a Mg,Al–LDH calcined at 560°C. Chatêlet et al. [228] have found that the amount of chromate adsorbed on a Mg,Al–LDH calcined at 450°C is larger than its anionic exchange capacity (AEC), with a change in the shape of the adsorption isotherm exactly at a value corresponding to such AEC. These authors conclude that adsorption above the AEC takes place on external sites with partially variable charge and, from specific surface area measurements, conclude that the surface density of adsorbed chromate is ca. 1 nm^2, a value fairly close to the average value of site density on oxides [229].

The ability of Mg,Al–LDH to adsorb TcO_4^{2-} and ReO_4^{2-} has been studied to test their applicability for removal of Tc^{7+} from radioactive wastes [230]. The sorption has been found to lead to grafted intercalates, substituting one or two hydroxyl groups from the layers, depending on the TcO_4^{2-}/LDH ratio.

Similar studies have been also reported by Yamagishi et al. [231] on the adsorption of chromate and permanganate on a thermally decomposed Mg,Al–LDH. The intercalates, with a basal spacing of 8.7 Å, are then calcined at 800–900°C to avoid leaching of the heavy cations to aqueous solutions.

The strong basicity of hydrotalcites provides unexpected properties to modulate the catalytic properties of supported catalysts. Pinnavaia et al. [232] have supported $Ru_3(CO)_{12}$ on a Mg,Al–LDH by suspending the hydrotalcite in a degassed CH_2Cl_2 solution of the carbonyl complex. This undergoes reductive decarbonylation to the $HRu_3(CO)_{11}^-$, as confirmed by IR spectroscopy; equivalent reductive decarbonylation in homogeneous solution requires the presence of very strong bases [233], provided in the LDH by hydrolysis of the carbonate anion. After exposure to air, oxidation leads to grafted $[Ru(CO)_x(OM\equiv)_2]_n$, analogous to grafted cationic complexes formed on aluminum-pillared montmorillonite [234]. Reduction at 275°C yields Ru crystallizes active for Fischer-Tropsch reaction, forming a high fraction of oxygenates (mainly methanol and lesser amounts of C_2–C_4 alcohols).These authors [232] propose decoration of the metal crystallizes by the basic support to explain oxygenates formation.

As with complexes of macrocyclic ligands, photophysical properties of other anionic photocatalysts may be also modified when intercalated in LDHs. Pinnavaia et al. [67] have reported immobilization of the luminescent anion $Ru(BPS)_3^{4-}$ (BPS = 4,7-diphenyl-1,10-phenantrolinedisulphonate) in a Mg,Al–LDH. Incomplete chloride exchange led to a layered material with a basal spacing of 22 Å, indicating the complex is intercalated with its C_3 axes normal to the layers.

Although marginal perturbations in the visible absorption profile are similar to those observed for $Ru(bipy)_3^{2+}$ intercalated in smectite clays, the IR and Raman spectra of intercalated $Ru(BPS)_3^{4-}$ and in solution are almost coincident, thus discarding such low-symmetry-ligand distortions. The luminescence decay is complex, a behavior that in the case of smectites has been ascribed to quenching of the excited state by impurity ions (e.g. Fe^{3+}, Cr^{3+}) isomorphically substituting Al^{3+} or Si^{4+} in the clay structure [235], but this is precluded in the LDH. On the contrary, the multiphasic emission decay in hydrotalcites arises from self-quenching, as these authors have concluded from studies with systems simultaneously containing $Ru(BPS)_3^{4-}$ and nonemissive $Zn(BPS)_3^{4-}$.

CdS and CdS–ZnS have been incorporated into the interlayer of a Mg,Al–LDH [236] and their photocatalytic properties for hydrogen evolution from Na_2S, Na_2SO_3 and/or 2-aminoethanol [237] under visible light ($\lambda > 400$ nm) irradiation has been studied. The particle size of CdS should be very small (ca. 1 nm), as the band gap of the Mg,Al–LDH/CdS was 2.64 eV, slightly larger than that of unsupported CdS (2.40 eV), while for alloyed CdS–ZnS it was even smaller. The photoactivity in the named reaction was larger for intercalated $Cd_{1-x}Zn_xS$ than for the corresponding, unsupported sol, although the use of semiconducting supports (e.g. $H_2Ti_4O_9$ or $H_4Nb_6O_{17}$) further improved the photoactivity.

5. Conclusions

From the results in this review, it is obvious the interest that layered double hydroxides have deserved in recent years. Its structure, similar to that of layered silicates, but with a change in the sign of the electric charges of the layers and the interlayer ions, makes them true companions in systematizing the study of these solids. On the other hand, as the layer cations and the interlayer anions can be almost chosen from any one in the Periodic Table, the opportunities for synthesis chemistry are enormous. This obviously constitutes a challenge for chemists. In addition, the promising role that these materials, as obtained or after adequate thermal treatments, can play as catalysts, sensors, electrodes, etc., makes them worthwhile to be studied in a systematic way to modulate and to improve their properties. Probably, in the next few years we will witness a lot of new work on these compounds, expanding the nature of intercalated metal-containing anions.

Acknowledgements

The authors would like to thank the collaboration of their co-workers in the Universities of Córdoba and Salamanca (Spain), as well as of Dr W. Jones (University of Cambridge, UK), Dr P. Malet (Universidad de Sevilla, Spain), and Dr F. Kooli (currently at NIRIM, Tsukuba, Japan). Finantial support by Junta de Castilla y León (Consejería de Educación y Cultura, grant SA45/96), Junta de Andalucía (grant FQM-214) and Ministerio de Educacion y Cultura (grant PB96-1307-C03) is acknowledged.

References

[1] A. de Roy, C. Forano, K. El Malki, J.-P. Besse, in: M.L. Occelli, H.E. Robson (Eds.), Synthesis of Microporous Materials, vol. 2, Expanded Clays and Other Microporous Systems, Van Nostrand Reinhold, New York, 1992, pp. 108–169.

[2] F. Trifirò, A. Vaccari, in: J.L. Atwood, J.E.D. Davies, D.D. MacNicol, F. Vögtle, J.-M. Lehn, G. Alberti, T. Bein (Eds.), Comprehensive Supramolecular Chemistry, vol. 7, Solid-State Supramolecular Chemistry: Two- and Three-Dimensional Inorganic Networks, Pergamon, Oxford, 1996, pp. 251–291.

[3] F. Cavani, F. Trifirò, A. Vaccari, Catal. Today 11 (1991) 173.

[4] M. Zikmund, K. Hrnciarová, Chem. Listy 91 (1997) 169.

[5] W.T. Reichle, Solid State Ionics 22 (1986) 135.

[6] M. Chibwe, J.B. Valim, W. Jones, in: C.A.C. Sequeira, M.J. Hudson (Eds.), Multifunctional Mesoporous Solids, Kluwer, Amsterdam, 1993, pp. 191–206.

[7] K.A. Carrado, A. Kostapapas, S.L. Suib, Solid State Ionics 26 (1988) 77.

[8] M. Meyn, K. Beneke, G. Lagaly, Inorg. Chem. 29 (1990) 5201.

[9] W. Jones, M. Chibwe, in: I.V. Mitchell (Ed.), Pillared Layered Structures: Current Trends and Applications, Elsevier, London, 1990, pp. 67–77.

[10] R.M. Taylor, Clay Miner. 19 (1984) 591.

[11] S. Velu, V. Ramaswamy, A. Ramani, B.M. Chanda, S. Sivasanker, J. Chem. Soc. Chem. Commun. (1997) 2107.

[12] C.J. Serna, J.L. Rendón, J.E. Iglesias, Clays Clay Miner. 10 (1982) 180.

[13] M.A. Drezdzon, ACS Symp. Ser. 437 (1990) 140.

[14] A. Clearfield, M. Kuchenmeister, J. Wang, K. Wade, in: P.A. Jacobs, N.I. Jaeger, L. Kubelková, B. Wichterlová (Eds.), Zeolite Chemistry and Catalysis, Elsevier, Amsterdam, Stud. Surface Sci. Catal., vol. 69, 1991, pp. 485–497.

[15] A. Clearfield, in: C.A.C. Sequeira, M.J. Hudson (Eds.), Multifunctional Mesoporous Solids, Kluwer, Amsterdam, 1993, pp. 159–178.

[16] S. Yamanaka, Mater. Sci. Forum 152–153 (1994) 69.

[17] K. Ohtsuka, Chem. Mater. 9 (1997) 2039.

[18] R. Szostak, C. Ingram, in: H.K. Beyer, H.G. Karge, I. Kiricsi, J.B. Nagy (Eds.), Catalysis by Microporous Materials, Elsevier, Amsterdam, Stud. Surface Sci. Catal., vol. 94, 1995, pp. 13–38.

[19] T.J. Pinnavaia, M. Chibwe, V.R.L. Constantino, S.K. Yun, Appl. Clay Sci. 10 (1995) 117.

[20] A. Corma, Chem. Rev. 97 (1997) 2373.

[21] E. López-Salinas, Y. Ono, Microporous Mater. 1 (1993) 33.

[22] A.B.P. Lever, E. Montovani, B.S. Ramaswany, Can. J. Chem. 49 (1971) 1957.

[23] L.E. Alzamora, J.R.H. Ross, E.C. Kruissink, L.L. van Reijden, J. Chem. Soc. Faraday Trans. I 77 (1981) 665.

[24] J.R. Weisner, R.C. Srivastava, C.H.L. Kennard, M. di Vaira, E.C. Lingafelter, Acta Crystallogr. 23 (1967) 565.

[25] J. Brynestad, G.P. Smith, J. Am. Chem. Soc. 92 (1970) 3198.

[26] A.B.P. Lever, Inorganic Electronic Spectroscopy, 2nd edn, Elsevier, Amsterdam, 1984, p. 507.

[27] F.A. Cotton, D.M.L. Goodgame, M. Goodgame, J. Am. Chem. Soc. 83 (1961) 4690.

[28] K. Okada, F. Matsushita, S. Hayashi, Clay Min. 32 (1997) 299.

[29] E. López-Salinas, N. Tomita, T. Matsui, E. Suzuki, Y. Ono, J. Mol. Catal. 81 (1993) 397.

[30] E. López-Salinas, Y. Ono, E. Suzuki, Mater. Res. Symp. Proc. 368 (1995) 363.

[31] K. Itaya, H.-C. Chang, I. Uchida, Inorg. Chem. 26 (1987) 624.

[32] K. Chibwe, W. Jones, J. Chem. Soc. Chem. Commun. (1989) 926.

[33] S. Miyata, T. Hirose, Clays Clay Min. 26 (1978) 441.

[34] S. Kikkawa, M. Koizumi, Mater. Res. Bull. 17 (1982) 191.

[35] L.H. Jones, Inorg. Chem. 2 (1963) 777.

[36] F.M. Labajos, V. Rives, M.A. Ulibarri, Spectrosc. Lett. 24 (1991) 499.

[37] P.S. Braterman, C. Tan, J. Zhao, Mater. Res. Bull. 29 (1994) 1217.

[38] J.D. Wang, G. Serrette, Y. Tian, A. Clearfield, Appl. Clay Sci. 10 (1995) 103.
[39] P.K. Dutta, M. Puri, J. Phys. Chem. 93 (1989) 376.
[40] S. Idemura, E. Suzuki, Y. Ono, Clays Clay Min. 37 (1989) 553.
[41] H.G. Drickamer, S.C. Fung, G.K. Lewis Jr., Adv. High Pressure Res. 3 (1969) 1.
[42] M.J. Holgado, V. Rives, M.S. San Román, P. Malet, Solid State Ionics 92 (1996) 273.
[43] H.C.B. Hansen, C.B. Koch, Clays Clay Min. 42 (1994) 170.
[44] J.A. Olabe, H.O. Zerga, Inorg. Chem. 22 (1983) 4156.
[45] I. Crespo, C. Barriga, V. Rives, M.A. Ulibarri, Solid State Ionics 101–103 (1997) 729.
[46] E. Suzuki, S. Idemura, Y. Ono, Clays Clay Min. 37 (1989) 173.
[47] F.A.P. Cavalcanti, A. Schutz, P. Biloen, in: B. Delmon, P. Grange, P.A. Jacobs, G. Poncelet (Eds.), Preparation of Catalysts IV, Elsevier, Amsterdam, 1987, pp. 165–174.
[48] K.S.W. Sing, D.H. Everett, R.A.W. Haul, L. Moscou, J. Rouquerol, T. Sieminiewska, Pure Appl. Chem. 57 (1985) 603.
[49] J.M. Fernández, M.A. Ulibarri, F.M. Labajos, V. Rives, J. Mater. Chem. 8 (1998) 2507.
[50] H. Nijs, P. Cool, E.F. Vansant, Interface Sci. 5 (1997) 83.
[51] G. Mao, M. Tsuji, Y. Tamaura, Clays Clay Min. 41 (1993) 731.
[52] D.W. Breck, W.G. Eversole, R.M. Milton, T.B. Reed, T.L. Thomas, J. Am. Chem. Soc. 78 (1956) 5963.
[53] T. Challier, R.C.T. Slade, J. Mater. Chem. 4 (1994) 367.
[54] B.R. Shaw, Y. Deng, F.E. Strillacci, K.A. Carrado, M.G. Fessehaie, J. Electrochem. Soc. 137 (1990) 3136.
[55] J. Labuda, M. Hudáková, Electroanalysis 9 (1997) 239.
[56] (a) J. Qiu, G. Villemure, J. Electroanal. Chem. 395 (1995) 159. (b) J. Qiu, G. Villemure, J. Electroanal. Chem. 428 (1997) 165.
[57] A. Cervilla, A. Corma, V. Fornés, E. Llopis, P. Palanca, F. Rey, A. Ribera, J. Am. Chem. Soc. 116 (1994) 1595.
[58] A. Cervilla, E. Llopis, A. Ribera, A. Corma, V. Fornés, F. Rey, J. Chem. Soc. Dalton Trans. (1994) 2953.
[59] A. Corma, V. Fornés, F. Rey, A. Cervilla, E. Llopis, A. Ribera, J. Catal. 152 (1995) 237.
[60] A. Corma, F. Rey, J.M. Thomas, G. Sankar, G.N. Greaves, A. Cervilla, E. Llopis, A. Ribera, J. Chem. Soc. Chem. Commun. (1996) 1613.
[61] P. Palanca, T. Picher, V. Sanz, P. Gómez-Romero, E. Llopis, A. Doménech, A. Cervilla, J. Chem. Soc. Chem. Commun. (1990) 531.
[62] V. Sanz, T. Picher, P. Palanca, E. Llopis, J.A. Ramírez, D. Beltrán, A. Cervilla, Inorg. Chem. 30 (1990) 3113.
[63] E. Llopis, A. Doménech, J.A. Ramírez, A. Cervilla, P. Palanca, T. Picher, V. Sanz, Inorg. Chim. Acta 189 (1991) 29.
[64] H. Kominami, S. Kurimoto, M. Kubota, R. Shiozaki, Y. Kera, J. Ceram. Soc. Jpn. 105 (1997) 707 (in Japanese).
[65] M.A. Drezdzon, Inorg. Chem. 27 (1988) 4628.
[66] M.D. Newsham, E.P. Giannelis, T.J. Pinnavaia, D.G. Nocera, J. Am. Chem. Soc. 110 (1988) 3885.
[67] E.P. Giannelis, D.G. Nocera, T.J. Pinnavaia, Inorg. Chem. 26 (1987) 203.
[68] P.K. Ghosh, A.J. Bard, J. Phys. Chem. 88 (1984) 5519.
[69] R.A. Della Guardia, J.K. Thomas, J. Phys. Chem. 87 (1983) 990.
[70] H. Nijs, J.J. Fripiat, H. Van Damme, J. Phys. Chem. 87 (1983) 1279.
[71] J.R. Winkler, H.B. Gray, J. Am. Chem. Soc. 105 (1983) 1373.
[72] S. Miyata, A. Okada, Clays Clay Min. 25 (1977) 14.
[73] (a) S. Miyata, Clays Clay Min. 23 (1975) 369. (b) S. Miyata, Clays Clay Min. 31 (1983) 305.
[74] J.R. Winkler, H.B. Gray, Inorg. Chem. 24 (1985) 346.
[75] L. Barloy, J.P. Lallier, P. Battioni, D. Mansuy, Y. Piffard, M. Tournous, J.B. Valim, W. Jones, New J. Chem. 16 (1992) 71.
[76] M.E. Pérez–Bernal, R. Ruano-Casero, T.J. Pinnavaia, Catal. Lett. 11 (1991) 55.
[77] S. Fukuzumi, S. Mochizuki, T. Tanaka, Isr. J. Chem. 23 (1987–1988) 29.
[78] L. Gaillon, F. Bedioui, J. Devinck, P. Battioni, J. Electroanal. Chem. 347 (1993) 435.

[79] H. Van Damme, M. Crespin, F. Obrecht, M.I. Cruz, J.J. Fripiat, J. Colloid Interface Sci. 66 (1978) 43.
[80] H. Kameyama, H. Suzuki, A. Amano, Chem. Lett. (1988) 1117.
[81] C. Mousty, S. Therias, C. Forano, J.P. Besse, J. Electroanal. Chem. 374 (1994) 63.
[82] S. Therias, C. Mousty, Appl. Clay Sci. 10 (1995) 147.
[83] J. Martinsen, J.L. Stanton, R.L. Greene, J. Tanaka, B.M. Hoffman, J.A. Ibers, J. Am. Chem. Soc. 107 (1985) 6915.
[84] T.J. Pinnavaia, Adv. Chem. Ser. 245 (1995) 283.
[85] F. Bedioui, Coord. Chem. Rev. 144 (1995) 39.
[86] I.Y. Park, K. Kuroda, C. Kato, Chem. Lett. (1989) 2057.
[87] K. Sakoda, K. Kominami, M. Iwamoto, Jpn. J. Appl. Phys. 27 (1988) L1304.
[88] S. Bonnet, L. Bigey, C. Forano, A. de Roy, J.P. Besse, P. Maillard, M. Momenteau, in: M.L. Occelli, H. Kessler (Eds.), Synthesis of Porous Materials: Zeolites, Clays and Nanostructures, Marcel Dekker, New York, 1997, pp. 627–640.
[89] S. Bonnet, C. Forano, A. de Roy, J.P. Besse, P. Maillard, M. Momenteau, Chem. Mater. 8 (1996) 1962.
[90] A. Stone, E.B. Fleisher, J. Am. Chem. Soc. 90 (1968) 2735.
[91] H. Tagaya, A. Ogata, T. Kuwahara, S. Ogata, M. Karasu, J. Kadokawa, K. Chiba, Microporous Mater. 7 (1996) 151.
[92] R.A. Schoonheydt, L. Heughebaert, Clay Miner. 27 (1992) 91.
[93] M. Chibwe, T.J. Pinnavaia, J. Chem. Soc. Chem. Commun. (1993) 278.
[94] M. Chibwe, L. Ukrainczyk, S.A. Boyd, T.J. Pinnavaia, J. Mol. Catal. A: Chem. 113 (1996) 249.
[95] K.A. Carrado, J.E. Forman, R.E. Botto, R.E. Winans, Chem. Mater. 5 (1993) 472.
[96] I.Y. Park, K. Kuroda, C. Kato, J. Chem. Soc. Dalton Trans. (1990) 3071.
[97] I.J. Shannon, T. Maschmeyer, G. Sankar, J.M. Thomas, R.D. Oldroyd, M. Sheehy, D. Madill, A.M. Waller, R.T. Townsend, Catal. Lett. 44 (1997) 23.
[98] V.I. Iliev, A.I. Ileva, L.D. Dimitrov, Appl. Catal. A: Gen. 126 (1995) 333.
[99] V. Iliev, J. Mol. Catal. 85 (1993) L269.
[100] J.M. Assour, W.K. Kahn, J. Am. Chem. Soc. 87 (1965) 207.
[101] J.F. Boas, P.E. Fielding, A.G. McKay, Austr. J. Chem. 27 (1974) 7.
[102] V. Iliev, A. Andreev, D. Wohrle, G. Schulz-Ekloff, J. Mol. Catal. 66 (1991) L5.
[103] A. Skorobogaty, T.D. Smith, J. Mol. Catal. 16 (1982) 131.
[104] J. Zwart, H.C. van der Weide, N. Broeker, C. Rummens, G.C.A. Schuit, A.L. German, J. Mol. Catal. 3 (1977–1978) 151.
[105] L. Ukrainczyk, M. Chibwe, T.J. Pinnavaia, S.A. Boyd, J. Phys. Chem. 98 (1994) 2668.
[106] R. Allmann, Chimia 24 (1970) 99.
[107] M.B. McBride, Clays Clay Miner. 27 (1979) 97.
[108] E.P. Giannelis, Chem. Mater. 2 (1990) 627.
[109] J. Subramanian, in: K.M. Smith (Ed.), Porphyrins and Metalloporphyrins, Elsevier, Amsterdam, 1975, p. 568.
[110] L. Ukrainczyk, M. Chibwe, T.J. Pinnavaia, S.A. Boyd, Environ. Sci. Technol. 29 (1995) 439.
[111] U.E. Krone, R.K. Thauer, H.P.C. Hogenkamp, Biochemistry 28 (1989) 4908.
[112] U.E. Krone, K. Laufer, R.K. Thauer, H.P.C. Hogekamp, Biochemistry 28 (1989) 10061.
[113] C.J. Gantzer, L.P. Wackett, Environ. Sci. Technol. 25 (1991) 715.
[114] N. Assaf-Amid, K.F. Hayes, T.M. Vogel, Environ. Sci. Technol. 28 (1994) 246.
[115] G.M. Klecka, S.J. Gonsior, Chemosphere 3 (1984) 391.
[116] Y.C. Yang, J.R. Ward, R.P. Seiders, Inorg. Chem. 24 (1985) 1765.
[117] M. Zikmund, K. Putyera, K. Hrnciarova, Chem. Papers 50 (1996) 262.
[118] L. Gaillon, F. Bedioui, J. Devynck, P. Battioni, J. Electroanal. Chem. 347 (1993) 435.
[119] D.S. Robins, P.K. Dutta, Langmuir 12 (1996) 402.
[120] R.F. Pasternack, L. Francesconi, D. Raff, E. Spiro, Inorg. Chem. 12 (1973) 2606.
[121] K. Kalyanasundaram, M. Naumann-Spallart, J. Phys. Chem. 86 (1982) 5163.
[122] J. Wang, Y. Tian, R.-C. Wang, J.L. Colón, A. Clearfield, in: R.L. Bedard, T. Bein, M.E. Davis, J. Garces, V.A. Maroni, G.D. Stucky (Eds.), Synthesis/Characterization and Novel Applications of Molecular Sieve Materials, Materials Research Society, Pittsburgh, 1991, pp. 63–80.

[123] T. Tatsumi, K. Yamamoto, Trans. Mater. Res. Soc. Jpn. 15 (1994) 141.
[124] C.W. Hu, Q.L. He, E.B. Wang, Progr. Nat. Sci. 6 (1996) 524.
[125] S. Miyata, T. Kumura, H. Hattori, K. Tanabe, Nippon Kagaku Zasshi 92 (1971) 514 (in Japanese).
[126] C. Misra, A.J. Perrotta, Clays Clay Min. 40 (1992) 145.
[127] K. El Malki, A. de Roy, J.P. Besse, Eur. J. Solid State Inorg. Chem. 26 (1989) 339.
[128] C. Depège, C. Forano, A. de Roy, J.P. Besse, Mol. Cryst. Liq. Cryst. 244 (1994) 161.
[129] L. Bigey, C. Depège, A. de Roy, J.P. Besse, J. Phys. IV France, C2, 7 (1997) 949.
[130] S. Yamanaka, T. Sako, K. Seti, M. Hattori, Solid State Ionics 53–56 (1992) 527.
[131] C. Forano, A. de Roy, C. Depège, M. Khaldi, F.Z. El Metoui, J.P. Besse, in: M.L. Occelli, H. Kessler (Eds.), Synthesis of Porous Materials: Zeolites, Clays and Nanostructures, Marcel Dekker, New York, 1997, pp. 607–625.
[132] E. Suzuki, Y. Ono, Bull. Chem. Soc. Jpn. 61 (1988) 1008.
[133] H. Shimada, K. Saito, Nippon Kagaku Kaishi (1997) 335 (in Japanese).
[134] T. Kwon, G.A. Tsigdinos, T.J. Pinnavaia, J. Am. Chem. Soc. 110 (1988) 3653.
[135] J. Twu, P.K. Dutta, J. Phys. Chem. 93 (1989) 7863.
[136] W.P. Griffith, T.D. Wolkins, J. Chem. Soc. A (1966) 1087.
[137] W.P. Griffith, P.J.B. Lesniak, J. Chem. Soc. A (1969) 1066.
[138] A. Bhattacharyya, D.B. Hall, T.J. Barnes, Appl. Clay Sci. 10 (1995) 57.
[139] J. Twu, P.K. Dutta, J. Catal. 124 (1990) 503.
[140] R. Gopal, C. Calvo, Acta Crystallogr. Sect. B 30 (1974) 2491.
[141] C. Depège, L. Bigey, C. Forano, A. de Roy, J.P. Besse, J. Solid State Chem. 126 (1996) 314.
[142] K.S. Han, L. Guerlou-Demourgues, C. Delmas, Solid State Ionics 84 (1996) 227.
[143] K.S. Han, L. Guerlou-Demourgues, C. Delmas, Solid State Ionics 98 (1996) 85.
[144] M. Doeuff, T. Kwon, T.J. Pinnavaia, Synthetic Metals 34 (1989) 609.
[145] G.M. Woltermann, US patent 4,454,244, Ashland Oil Co., June 12, 1984.
[146] C. Barriga, W. Jones, P. Malet, V. Rives, M.A. Ulibarri, Inorg. Chem. 37 (1998) 1812.
[147] J. Evans, M. Pillinger, J. Zhang, J. Chem. Soc. Dalton Trans. (1996) 2963.
[148] K. Chibwe, W. Jones, Chem. Mater. 1 (1989) 489.
[149] F. Kooli, W. Jones, Inorg. Chem. 34 (1995) 6237.
[150] F. Kooli, W. Jones, V. Rives, M.A. Ulibarri, J. Mater. Sci. Lett. 16 (1997) 27.
[151] F. Kooli, M.J. Holgado, V. Rives, S. San Roman, M.A. Ulibarri, Mater. Res. Bull. 32 (1997) 977.
[152] E. Narita, P. Kaviratna, T.J. Pinnavaia, Chem. Lett. (1991) 805.
[153] E. Narita, P.D. Kaviratna, T.J. Pinnavaia, J. Chem. Soc. Chem. Commun. (1993) 60.
[154] J. Wang, Y. Tian, R.-C. Wang, A. Clearfield, Chem. Mater. 4 (1992) 1276.
[155] F. Kooli, V. Rives, M.A. Ulibarri, W. Jones, Mater. Res. Soc. Symp. Proc. 371 (1995) 143.
[156] G. Mascolo, O. Marino, Miner. Mag. 43 (1980) 619.
[157] M.A. Ulibarri, F.M. Labajos, V. Rives, W. Kagunya, W. Jones, R. Trujillano, Mol. Cryst. Liq. Cryst. 244 (1994) 167.
[158] M.A. Ulibarri, F.M. Labajos, V. Rives, W. Kagunya, W. Jones, R. Trujillano, Inorg. Chem. 33 (1994) 2592.
[159] I.C. Chisem, W. Jones, J. Mater. Chem. 4 (1994) 1737.
[160] F. Kooli, V. Rives, M.A. Ulibarri, Inorg. Chem. 34 (1995) 5114.
[161] F. Kooli, V. Rives, M.A. Ulibarri, Mater. Sci. Forum. 152–153 (1994) 375.
[162] O. Clause, B. Rebours, E. Merlen, F. Trifiro, A. Vaccari, J. Catal. 133 (1992) 231.
[163] F. Kooli, V. Rives, M.A. Ulibarri, Inorg. Chem. 34 (1995) 5122.
[164] J. Guo, Q.Z. Jiao, G. Xiong, H.J. Lu, D.Z. Jiang, E.Z. Min, Chin. Chem. Lett. 7 (1996) 531.
[165] W. Kagunya, W. Jones, Appl. Clay Sci. 10 (1995) 95.
[166] V. Rives, F.M. Labajos, M.A. Ulibarri, P. Malet, Inorg. Chem. 32 (1993) 5000.
[167] P. Malet, J.A. Odriozola, F.M. Labajos, V. Rives, M.A. Ulibarri, Nucl. Instr. Methods Phys. Res. B 97 (1995) 16.
[168] F. Kooli, I. Crespo, C. Barriga, M.A. Ulibarri, V. Rives, J. Mater. Chem. 6 (1996) 1199.
[169] A. Corma, J.M. López-Nieto, N. Paredes, M. Pérez, Appl. Catal. 97 (1993) 159.
[170] A. Corma, J.M. López-Nieto, N. Paredes, Appl. Catal. 104 (1993) 161.

[171] M.A. Chaar, D. Patel, M.C. Kung, H.H. Kung, J. Catal. 105 (1987) 483.
[172] F. Roozeboom, J. Medema, P.J. Gellings, Z. Phys. Chem. (Wiesbaden) 111 (1978) 215.
[173] R.L. Coustumer, B. Taouk, M. le Meur, E. Payen, M. Guelton, J. Grimblot, J. Phys. Chem. 92 (1988) 1230.
[174] E. López Salinas, Y. Ono, Bull. Chem. Soc. Jpn. 65 (1992) 2465.
[175] F. Kooli, C. Martin, V. Rives, Langmuir 13 (1997) 2303.
[176] C. Delmas, Y. Borthomieu, J. Solid State Chem. 104 (1993) 345.
[177] M. Ménétrier, K.S. Han, L. Guerlou-Demourgues, C. Delmas, Inorg. Chem. 36 (1997) 2441.
[178] S. Onodera, Y. Ikegami, Inorg. Chem. 19 (1980) 615.
[179] M. del Arco, C. Martin, I. Martin, V. Rives, R. Trujillano, Spectrochim. Acta Part A 49 (1993) 1575.
[180] L. Pesic, S. Salipurovic, V. Markovic, D. Vucelic, W. Kagunya, W. Jones, J. Mater. Chem. 2 (1992) 1069.
[181] M. del Arco, M.V.G. Galiano, V. Rives, R. Trujillano, P. Malet, Inorg. Chem. 35 (1996) 6362.
[182] M. del Arco, V. Rives, R. Trujillano, P. Malet, J. Mater. Chem. 6 (1996) 1419.
[183] L. Lowenstein, Am. Miner. 39 (1954) 92.
[184] K. Fuda, K. Suda, T. Matsunaga, Chem. Lett. (1993) 1479.
[185] V. Rives, M.A. Ulibarri, A. Montero, Appl. Clay Sci. 10 (1995) 83.
[186] B.I. Intorre, A.E. Martell, J. Am. Chem. Soc. 82 (1960) 358.
[187] F. Rey, V. Fornés, J.M. Rojo, J. Chem. Soc. Faraday Trans. 88 (1992) 2233.
[188] T. Hibino, A. Tsunashima, Chem. Mater. 9 (1997) 2082.
[189] J. Twu, P.K. Dutta, Chem. Mater. 4 (1992) 398.
[190] D. Levin, S.L. Soled, J.Y. Ying, Chem. Mater. 8 (1996) 836.
[191] D. Levin, S.L. Soled, J.Y. Ying, ACS Symp. Ser. 622 (1996) 237.
[192] M.P. Pope, Heteropoly and Isopoly Oxometalates, Springer-Verlag, New York, 1983.
[193] C. Preyssler, Bull. Soc. Chim. Fr. 1 (1970) 30.
[194] T. Kwon, T.J. Pinnavaia, Chem. Mater. 4 (1989) 381.
[195] Y.Y. Liu, C.W. Hu, Z.P. Wang, J.Y. Zhang, E.B. Wang, Sci. China Ser. B Chem. 39 (1996) 86 (in Chinese).
[196] E.D. Dimotakis, T.J. Pinnavaia Jr., in: E.W. Corcoran Jr., M.J. Ledoux (Eds.), Synthesis and Properties of New Catalysts: Utilization of Novel Materials Components and Synthetic Techniques, Materials Research Society, Pittsburgh, 1990, pp. 77–80.
[197] E.D. Dimotakis, T.J. Pinnavaia, Inorg. Chem. 29 (1990) 2393.
[198] S.K. Yun, V.R.L. Constantino, T.J. Pinnavaia, Microporous Mater. 4 (1995) 21.
[199] H.C.B. Hansen, R.M. Taylor, Clay Miner. 26 (1991) 311.
[200] M.R. Weir, J. Moore, R.A. Kydd, Chem. Mater. 9 (1997) 1686.
[201] J. Guo, T. Sun, J.P. Shen, D.Z. Jiang, E.Z. Min, Chem. J. Chin. Univ. 16 (1995) 512 (in Chinese).
[202] E. Serwicka, P. Nowak, K. Bahranowski, W. Jones, F. Kooli, J. Mater. Chem. 7 (1997) 1937.
[203] R.N. Hua, Q.J. Shan, J.A. Gong, L.Y. Qu, Chem. J. Chin. Univ. 17 (1996) 1500 (in Chinese).
[204] R.N. Hua, Q.J. Shan, B.Z. Zhao, Y.H. Wang, B.L. Li, L.Y. Qu, Acta Chim. Sin. 55 (1997) 773 (in Chinese).
[205] R.S. Weber, P. Gallezot, F. Lefebvre, S.L. Suib, Microporous Mater. 1 (1993) 223.
[206] C.-W. Hu, Q.-L. He, Y.-H. Zhang, Y.-Y. Liu, Y.-F. Zhang, T.-D. Tang, J.-Y. Zhang, E.-B. Wang, J. Chem. Soc. Chem. Commun. (1996) 121.
[207] C.W. Hu, Y.Y. Liu, Z.P. Wang, E.B. Wang, Acta Chim. Sin. 55 (1997) 49 (in Chinese).
[208] C.W. Hu, X. Zhang, Q.L. He, E.B. Wang, S.W. Wang, Q.L. Guo, Transit. Metal Chem. 22 (1997) 197.
[209] E. López Salinas, P. Salas Castillo, Y. Ono, Mater. Res. Soc. Symp. Proc. 371 (1995) 163.
[210] S.K. Yun, T.J. Pinnavaia, Inorg. Chem. 35 (1996) 6853.
[211] R.G. Finke, M.V. Droege, P.J. Domaille, Inorg. Chem. 26 (1987) 3886.
[212] C. Rocchiccioli-Deltcheff, R. Thouvenot, R. Franck, Spectrochim. Acta Part A 32 (1976) 587.
[213] T. Kwon, T.J. Pinnavaia, J. Mol. Catal. 74 (1992) 23.
[214] J. Guo, Q.Z. Jiao, J.P. Shen, H.J. Lu, D. Liu, D.Z. Jiang, E.Z. Min, Acta Chim. Sin. 54 (1996) 357 (in Chinese).

[215] M.A. Drezdzon, in: R. Terry, K. Baker, L.L. Murrel (Eds.), Novel Materials in Heterogeneous Catalysis, American Chemical Society, Washington, DC, 1990, pp. 141–148.

[216] K. Putyera, J. Jagiello, T.S. Bandosz, J.A. Schwarz, J. Chem. Soc. Faraday Trans. 92 (1996) 1243.

[217] T. Tatsumi, K. Yamamoto, H. Tajima, H. Tominaga, Chem. Lett. (1992) 815.

[218] T. Tatsumi, H. Tajima, K. Yamamoto, H. Tominaga, in: L. Guczi, F. Solymosi, P. Teteny (Eds.), New Frontiers in Catalysis, Elsevier, Amsterdam, 1993, pp. 1703–1706.

[219] E. Gardner, T.J. Pinnavaia, Appl. Catal. A: Gen. 167 (1998) 65.

[220] C. Hu, Q. He, Y. Zhang, E. Wang, T. Okuhara, M. Misono, Catal. Today 30 (1996) 141.

[221] J. Guo, Q.Z. Jiao, J.P. Shen, D.Z. Jiang, G.H. Yang, E.Z. Min, Catal. Lett. 40 (1996) 43.

[222] X. Zheng, W. Yue, H. Heming, J. Dazben, in: H. Hattori, M. Misono, Y. Ono (Eds.), Acid-Base Catalysis II, Elsevier, Amsterdam, Stud. Surface Sci. Catal. 90 (1994) 279.

[223] W. Kagunya, Z. Hassan, W. Jones, Inorg. Chem. 35 (1996) 5970.

[224] B. Keita, A. Belhouari, L. Nadjo, J. Electroanal. Chem. 314 (1991) 345.

[225] B. Keita, A. Belhouari, L. Nadjo, J. Electroanal. Chem. 355 (1993) 235.

[226] T. Sato, T. Wakabayashi, M. Shimada, I&EC Prod. Res. Develop. 25 (1986) 89.

[227] S.W. Rhee, M.J. Kang, H. Kim, C.H. Moon, Environ. Tech. 18 (1997) 231.

[228] L. Châtelet, J.Y. Bottero, J. Yvon, A. Bouchelaghem, Colloids Surf. A. Physicochem. Eng. Asp. 111 (1996) 167.

[229] W. Stumm, J.J. Morgan, Aquatic Chemistry—An Introduction Emphasizing Chemical Equilibria in Natural Waters, 2nd ed., Wiley, New York, 1981, Ch. 5.

[230] M.J. Kang, S.W. Rhee, H. Moon, V. Neck, T. Fanghanel, Radiochim. Acta 75 (1996) 169.

[231] T. Yamagishi, Y. Oyanagi, E. Narita, Nippon Kagaku Kaishi, (1993) 329 (in Japanese).

[232] T.J. Pinnavaia, M. Rameswaran, E.D. Dimotakis, E.P. Giannelis, E.G. Rightor, Faraday Discuss. Chem. Soc. 87 (1989) 227.

[233] C.R. Eady, P.F. Jackson, B.F.G. Johnson, J. Lewis, M.C. Malatesta, M. McPartlin, J.H. Nelson, J. Chem. Soc. Dalton Trans. (1980) 383.

[234] E.P. Giannelis, E.G. Rightor, T.J. Pinnavaia, J. Am. Chem. Soc. 110 (1988) 3880.

[235] F. Bergaya, H. Van Damme, J. Chem. Soc. Faraday Trans. II 79 (1983) 505.

[236] T. Sato, H. Okuyama, T. Endo, M. Shimada, React. Solids 8 (1990) 63.

[237] T. Sato, K. Masaki, T. Yoshiaki, A. Okuwaki, J. Chem. Tech. Biotechnol. 58 (1993) 315.